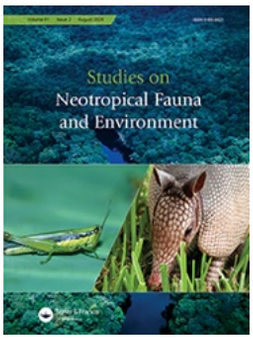

Studies on Neotropical Fauna and Environment

ISSN: 0165-0521 (Print) 1744-5140 (Online) Journal homepage: www.tandfonline.com/journals/nnfe20

Sedge feeders: early-stage biology of five Satyrinae butterflies (Lepidoptera: Nymphalidae) associated with Cyperaceae in southeastern Peru

Yeison Vega , Zunilda Escalante-Arteaga , Karla Fiallos-Yanez , Katherine García-Luquillas , Keith Willmott , Geoffrey Gallice & Shinichi Nakahara

To cite this article: Yeison Vega , Zunilda Escalante-Arteaga , Karla Fiallos-Yanez , Katherine García-Luquillas , Keith Willmott , Geoffrey Gallice & Shinichi Nakahara (10 Aug 2026): Sedge feeders: early-stage biology of five Satyrinae butterflies (Lepidoptera: Nymphalidae) associated with Cyperaceae in southeastern Peru, Studies on Neotropical Fauna and Environment, DOI: 10.1080/01650521.2026.2700355

To link to this article: https://doi.org/10.1080/01650521.2026.2700355

STUDIES ON NEOTROPICAL FAUNA AND ENVIRONMENT
https://doi.org/10.1080/01650521.2026.2700355

Sedge feeders: early-stage biology of five Satyrinae butterflies (Lepidoptera: Nymphalidae) associated with Cyperaceae in southeastern Peru

Yeison Vega [a], Zunilda Escalante-Arteaga [a], Karla Fiallos-Yanez [a], Katherine García-Luquillas [a,b], Keith Willmott [c,d,e], Geoffrey Gallice [f,g,h] and Shinichi Nakahara [i]

[a]Alianza para una Amazonía Sostenible Perú, Madre de Dios, Peru; [b]Laboratorio de Micología y Biotecnología, Universidad Nacional Agraria La Molina, Lima, Peru; [c]McGuire Center for Lepidoptera and Biodiversity, Florida Museum of Natural History, University of Florida, Gainesville, FL, USA; [d]Research Associate, Instituto Nacional de Biodiversidad, Quito, Ecuador; [e]Research Associate, National Museum of Natural History, Smithsonian Institution, Washington, DC, USA; [f]Departamento de Ingeniería, Pontificia Universidad Católica del Perú, Lima, Peru; [g]Alliance for a Sustainable Amazon, Potomac, MD, USA; [h]Department of Natural History, Florida Museum of Natural History, University of Florida, Gainesville, FL, USA; [i]Museum of Comparative Zoology and Department of Organismic and Evolutionary Biology, Harvard University, Cambridge, MA, USA

ABSTRACT

We describe the life cycles of four Neotropical satyr species feeding on Cyperaceae (sedges) in southeastern Peru: *Chloreuptychia chlorimene*, *Erichthodes antonina*, *Modica myncea*, and *Pierella hyalinus*. We report two sedge species, *Scleria secans* and a second unidentified *Scleria* species as natural host plants for these butterflies; we also report the latter as serving as the host plant for a fifth satyr species, *Magneuptychia libye*, for which the immature stages have been documented but for which this plant was not known as a natural host. Cyperaceae (sedges) are not commonly reported as host plants within the nymphalid butterfly subfamily Satyrinae, making this an interesting finding from both ecological and evolutionary perspectives. The larvae of all studied species exhibit cryptic coloration, suggesting possible adaptations to their host plants. Knowledge of the immature stages and host plant associations of the species here described may contribute to clarifying phylogenetic relationships within the group, as well as provide a foundation for future studies across multiple disciplines.

ARTICLE HISTORY
Received 12 March 2026
Accepted 29 June 2026

KEYWORDS
Amazon rainforest; Euptychiina; Haeterini; host plants; immature; natural history

Introduction

Despite major recent advances in biodiversity research, our understanding of many of its fundamental dimensions remains uneven, with substantial knowledge gaps persisting across multiple biological levels (Diniz-Filho et al. 2013). Important gaps in our knowledge relate to species description and categorization (Brown and Lomolino 1998), distribution (Lomolino 2004), abundance and population dynamics (Cardoso et al. 2011), phylogenetics (Diniz-Filho et al. 2013), and ontogeny (Faria et al. 2020). The last of these, the influence of ontogeny in structuring biodiversity, has been little explored, even in taxonomically well-established groups such as Lepidoptera. The lack of existing knowledge of the immature stages of organisms in hyperdiverse ecosystems, such as those of the Neotropics, amplifies other knowledge gaps, hindering our understanding of basic biological phenomena such as ecological interactions, the association between adults and early developmental stages, morphological evolution, and evolutionary history. In Lepidoptera, information from immature stages has proven informative in multiple studies in understanding their relationships and resolving species-level taxonomy (e.g. Kitching 1984; DeVries 1986; Penz and Peggie 2003; Freitas and Brown 2004; Hebert et al. 2004; Lin et al. 2019).

In recent decades, efforts to document the host plants and immature stages of Neotropical butterflies has made information available for several butterfly groups (e.g. Beccaloni et al. 2008; Janzen and Hallwachs 2018). However, we still lack basic knowledge of immature stages for the vast majority of species in many lineages, especially those that exhibit high diversity, taxonomic and systematic complexity, cryptic behaviors, and mimicry, among others. In Satyrinae butterflies, one of the most species-rich subfamilies (Ackery et al. 1999; Pyrcz and Wojtusiak 2002; Espeland et al. 2019), there has been an increase in studies focused on the description of the immature

CONTACT Yeison Vega yeison.vega@sustainableamazon.org
Supplemental data for this article can be accessed online at https://doi.org/10.1080/01650521.2026.2700355.

Published online 10 Aug 2026

stages, but the information currently available on host plants and life cycles for the Neotropical groups remains limited relative to the group's size and highly fragmented (e.g. Beccaloni et al. 2008).

Larvae of Satyrinae feed primarily on monocotyledons (Ackery 1988; Beccaloni et al. 2008), with the majority of species of the tribe Satyrini utilizing various Poaceae species as host plants (Beccaloni et al. 2008) as well as species in the families Arecaceae, Marantaceae, Heliconiaceae, Commelinaceae, Selaginellaceae, Neckeraceae, and Cyperaceae (DeVries 1987; Singer and Ehrlich 1991; Murray 2001; Janzen and Hallwachs 2018). Although rare, records of Cyperaceae as host plants within Satyrinae encompasses several tribes and include species of *Caligo* Hübner, [1819] (Brassolini) (Otero and Marigo 1990; Brown 1992; Otero and Casagrande 1992) and *Eryphanis* Boisduval, 1870 (Brassolini) (Brown 1992), *Pierella nereis* (Drury, 1782) (Haeterini) (Brown 1992), and several species within the subtribe Euptychiina. However, some of these records in the Satyrini represent feeding on plants offered in captivity (e.g. DeVries 1986; Singer and Ehrlich 1991; Brown 1992; Zacca et al. 2020), making it unclear whether these plants are used naturally by the species studied.

In the present study, we address the above-mentioned knowledge gap by providing a detailed description of the immature stages of four satyr species associated with Cyperaceae host plants in southeastern Peru: *Chloreuptychia chlorimene* (Hübner, [1819]), *Erichthodes antonina* (C. Felder and R. Felder, 1867), *Modica myncea* (Cramer, 1780) (Euptychiina), and *Pierella hyalinus* (Gmelin, [1790]) (Haeterini). We also document the use of *Scleria* as a host plant for *Magneuptychia libye* (Linnaeus, 1767) (Euptychiina). Additionally, we document several notable findings related to the immature biology of these species, including previously undocumented intraspecific variation in larval instars and pupal morphology. Finally, we compared the morphology with related species and genera, and discussed the potential implications for the phylogenetic hypotheses proposed in previous studies.

Materials and methods

Study site and field collection

This study was carried out at the Finca Las Piedras field station (FLP) located in the Madre de Dios department in southeastern Peru (12°13'40'S; 69°6'40' W, 240 m asl). FLP consists of 74 ha of mostly *terra firme* or upland rainforest dominated by Brazil nut *Bertholletia excelsa* Humb. and Bonpl. (Lecythidaceae) and other emergent hardwood species, although swamps ('aguajales' locally) dominated by the palm *Mauritia flexuosa* L. (Arecaceae) and areas of both agriculture and regenerating secondary forest are on the property or nearby (for more information about FLP, including tree species composition, see Fortier et al. 2025). Immatures were collected by searching potential Cyperaceae hosts at FLP and subsequently transported from the field to the onsite laboratory for rearing to adulthood under controlled conditions. The collection of specimens was authorized by Peru's Servicio Nacional Forestal y de Fauna Silvestre (SERFOR; research permit number D000443-2021-MIDAGRI-DGGDPFFS). This project is part of a long-term initiative to document the diversity and biology of Lepidoptera in southeastern Peru conducted by the Alliance for a Sustainable Amazon (ASA).

Rearing

Immature specimens collected in the field were brought to the laboratory for monitoring in 1 L plastic containers covered with fine nylon mesh cloths and held tightly in place with rubber bands. The host plant leaves were kept hydrated by placing the leaf petioles inside floral water tubes and were replaced as needed to ensure that the larvae had fresh leaves to feed on. Each individual was assigned a unique voucher (2025-FLP-IMM-0012, 2024-FLP-IMM-0813) used throughout the text and tables and monitored daily for important life events, which were recorded (e.g. molt dates by checking for discarded head capsules, whether or not the plant was fed). Immatures were photographed daily using a Nikon D7100 digital camera and Nikon AF-S VR Micro-NIKKOR 105 mm f/2.8 G IF-ED lens. All photographs included a scale in mm for subsequent measurements by pixel counting using ImageJ 1.54d (Schneider et al. 2012). Emerged adults were papered or mounted and stored in the ASA's biological collections in Puerto Maldonado, Peru (ASA).

Specimen identification

The identification of adult butterflies was carried out by comparing them with images of type specimens available on the Butterflies of America website (https://www.butterfliesofamerica.com), with the exception of *C. chlorimene*, which was identified based on the original watercolor illustrations of *Papilio chloris* Cramer, 1780 produced by Gerrit Wartenaar Lambertz [1747–1803] (on pl. 268, Figure A) (from the Library and Archives collections of the Natural History Museum, London). Species-level

identification within the Euptychiina was performed using neighbor-joining clustering analyses on alignments of DNA barcodes (Data analysis section). Plant identifications were initially conducted at the genus level by comparison with herbarium material available digitally on Tropicos.org, the collections of the Field Museum, and Kew Gardens, and were subsequently corroborated with Isabel Larridon, Kenneth Bauters, and Gordon C. Tucker, botanists specialized in Cyperaceae. The plant identified as *Scleria* sp. could not be determined to species level.

Morphology

Measurements for all life stages were made by counting pixels calibrated to scale in high resolution digital photographs using ImageJ 1.54d (Schneider et al. 2012). Measurements included the maximum diameter of the egg and length of the larvae and pupa taken in dorsal view from the anterior portion of the head to posterior margin of the tenth abdominal segment. Examination and photography of head capsules were carried out using a Leica S9D stereomicroscope with a View 4K HD Camera, and subsequently illustrated with Krita 5.2.11 software. The width of the head capsule was considered as the distance between the most external stemmata. The description of the egg followed the works of García-Barros and Martín (1995); the approach of Stehr (1987) and Murray (2001) was followed for the larvae and pupa description.

Molecular work

COI (mitochondrial cytochrome c oxidase I gene) barcode sequences were obtained in the molecular laboratory at FLP for selected specimens to test for conspecificity among dead larvae and to generate genetic information for ongoing and future studies. Genomic DNA was extracted from a single leg from each specimen using the boiling method described by Shin et al. (2021) with a modified TE buffer (10 mM Tris-Cl, 0.5 mM EDTA, pH 9.0). To permit multiplexing of multiple samples, the primers LCO1429 and HCO2198 (Folmer et al. 1994) were synthesized with different 9-bp tags at the 5' ends following the protocol of Srivathsan and Meier (2024), such that each specimen had a unique combination of forward and reverse 9-bp tags. Each PCR reaction was performed in a total volume of 12.5 µL containing 1.25 µL of 10x High Fidelity buffer, 0.5 µL of 50 mM $MgSO_4$, 0.25 µL of 10 mM dNTPs, 0.06 µL of 5 U/µL Platinum Taq High Fidelity DNA Polymerase (Thermo Fisher Scientific), 0.3 µL of 20 mg/mL molecular biology grade recombinant albumin (New England Biolabs), 7.64 µL of molecular grade water, 0.25 µL of forward and 0.25 µL reverse tagged primers (10 µM), and 2 µL of DNA template. The thermal cycling profile consisted of an initial denaturation step at 94°C for 1 min, followed by 5 cycles of 94°C for 30 s, 48°C for 40 s, and 68°C for 1 min; then 35 cycles of 94°C for 30 s, 52°C for 40 s, and 68°C for 1 min; and a final extension at 68°C for 10 min. Successful amplification was verified for a subset of samples using electrophoresis on 1.5% agarose gels with 1x TBE buffer, 6X TriTrack DNA loading dye (Thermo Fisher Scientific), a 100 bp DNA ladder, and XpertGreen DNA Stain (GRISP Research Solutions). Electrophoresis was conducted on a blueGel electrophoresis system (miniPCR Bio) under default settings (60 V) for 45 min. Library preparation was performed by pooling 8 µL of each uniquely tagged amplicon, following the MinION Ligation Sequencing Kit V14 protocol (Oxford Nanopore Technologies), with modifications following Srivathsan and Meier (2024). Sequencing was carried out on the MinION M1kB device using a FLO-MIN114 Flow Cell. Sequences were obtained using the high-accuracy Nanopore basecalling model (HAC), and ONTbarcoder 2.3.0 software (Srivathsan et al. 2023) was subsequently used to demultiplex sequences from the pooled samples.

Data analysis

A search for additional COI sequences was conducted in GenBank for *E. antonina*, *M. myncea*, *C. chlorimene*, and related Euptychiina species (Supplementary Table S3). COI sequence alignment was performed with MAFFT v7 using the online service and the G-INS-1 iterative refinement method (Katoh et al. 2019). The alignment was checked and trimmed to a uniform length using AliView (Larsson 2014). To graphically illustrate taxa, a neighbor-joining analysis was performed using MEGA 7.0 (Kumar et al. 2016), employing the Kimura two-parameter substitution model, partial deletion of sites with missing data, 1000 bootstrap replicates, and all other parameters set to default values. GenBank accession numbers for sequenced samples are listed in Supplementary Table S3.

Results

All recorded molting dates and voucher codes associated with individuals are provided in Supplementary Table S1. Information related to the position at which the immatures were collected, as well as characteristics of the plant, are provided in Supplementary Table S2. Euptychiina species descriptions are ordered

phylogenetically following Espeland et al. (2023), followed by the new host plant record of *M. libye*, and closing with the description of immature stages of *P. hyalinus*. Morphological identification and DNA barcode-based identification was congruent in all cases, including dead larvae, grouping the specimens into the corresponding clades with high bootstrap support (Supplementary Figure S1). We highlight the possibility that *C. chlorimene* may constitute a species complex (Supplementary Figure S1); therefore, the name used here should be considered provisional pending future taxonomic revisions of the genus.

Description of immature stages

Chloreuptychia chlorimene (Hübner, [1819])

Vouchers. 2025-FLP-IMM-0015, 0016, 0022, 0064, 0065, 0074, 0075, 0091, 0092, 0093, 0105 (GenBank accession numbers: PZ007833, PZ007834, PZ007835).

Egg (Figure 1A, B, C). Spherical, shiny, pearl-like and yellowish, in some individuals more whitish. Chorion surface cells not discernible based on photographs. Head capsule visible day prior to hatching. Diameter: 0.67–0.73 mm ($n = 3$). Duration: Unknown, hatched 3–4 days after collection ($n = 4$).

First instar (Figure 1D, E). Head capsule width: 0.42–0.44 mm ($n = 3$). Head capsule (Figure 2A) black to dark brown, shiny, faint, barely noticeable striations arranged in regular hexagons, with two short subrectangular scoli (scolus length: 0.49 mm; $n = 2$), each bearing two broad setae, one at each end. Three chalazae visible on each side in dorsal view, M1, M2, M3, additionally P1, P2, and P4 chalazae present, all with thick black seta. Six setae visible on one side of labrum. Six visible stemmata, with stemma 2 and 3 larger, but stemma 3 largest and closer to stemma 2 than 4, stemma 1 and 6 somewhat semi-transparent and thus insignificant. Body integument creamy-yellowish and semi-transparent, dark green from T1 up to A5 after feeding, two grayish mid-dorsal bands, a grayish subdorsal band, and a grayish supra-spiracular band extending from T1 to A3. Short, slightly bulbous, and thick setae throughout body, slightly longer from A8 to A10. Bifid caudal filaments, short, slightly yellow ending in a long, thick black seta. Body length: 5.2–5.3 mm ($n = 2$). Duration: 3–4 days ($n = 3$).

Second instar (Figure 1F, G). Head capsule width: 0.52–0.56 mm ($n = 2$). Head capsule (Figure 2B) black, matt, and pitted sculpting, whitish chalazae M1, M2, M3, P1, P2, and P4, with three whitish, smaller elongated setal bases between M1 in dorsal view. Scoli developed and appearing horn-like, oriented forward and with multiple elongated setal bases on posterior side and between each scolus (scolus length: 0.24 mm; $n = 1$), one setal base whitish near P1 and another on base of scolus. Elongated setal bases near to stemmata 2 and 3 elongated and whitish. Each setal base and chalaza ends in a black, short seta. Body light green, mid-dorsal line slightly darker, with yellowish micro-granulations across body. Two yellowish lines, one in subdorsal and another in supra-spiracular region. Bifid caudal filaments, slightly pinkish on inner side and whitish on outer side. Body length: 8.6–8.7 mm ($n = 2$). Duration: 4–5 days ($n = 2$).

Third instar (Figure 1H, I). Head capsule width: 0.60–0.72 mm ($n = 2$). Head capsule (Figure 2C) dark brown with creamy band and chalazae between M1 and behind scoli. Head capsule with pitted sculpting. Chalazae and elongated setal bases similar in shape and color to previous instar, but with additional elongated setal bases near to stemmata 2 and 3, and more evident. Scoli similar to previous instar, but slightly longer and with greater number of elongated setal bases on posterior side. As instar progresses, head capsule becomes slightly darker. Body similar to immediately preceding instar, but mid-dorsal line is more evident, and yellowish subdorsal line wider. Bifid caudal filaments more pinkish than previous instar. Body length: 12.0–12.6 mm ($n = 2$). Duration: 5 days ($n = 2$).

Fourth instar (Figure 1J, K). Head capsule width: 0.72–0.96 mm ($n = 4$). Shortly after molting, head capsule light green (Figure 2D); as instar progresses, it acquires light brown-reddish coloration, and it is more elongated, similar texture, and color patterns to immediately preceding instar. Scoli longer than in immediately preceding instar (scolus length: 0.66 mm; $n = 1$) and slightly pinkish. Body similar to previous instar except for subdorsal bands are slighter. Body length: 18.2–20.8 mm ($n = 2$). Duration: 6 days ($n = 1$).

Fifth instar (Figure 1L, M). Head capsule width: 0.84–1.36 mm ($n = 5$). Head capsule (Figure 2E) dark green with yellowish chalazae and elongated setal bases, and pitted sculpting. Three yellowish elongated setal bases near to stemmata 2 and 3. Chalazae yellowish and reduced, elongated setal bases D1, D2, and D3 reduced and barely noticeable. Scoli developed, appearing horn-like and pinkish, longer and thinner than immediately preceding instar. A yellowish line behind scoli. Multiple translucent setae near clypeus and mandibles. Body is similar to immediately preceding instar, but with dark gray mid-dorsal line from T1 to T3, thin-discontinuous green mid-dorsal zigzag longitudinal line from A3 to A10, and pair yellowish mid-dorsal lines from T3 to A10, subdorsal line turquoise, wider than previous instar and with whitish micro-

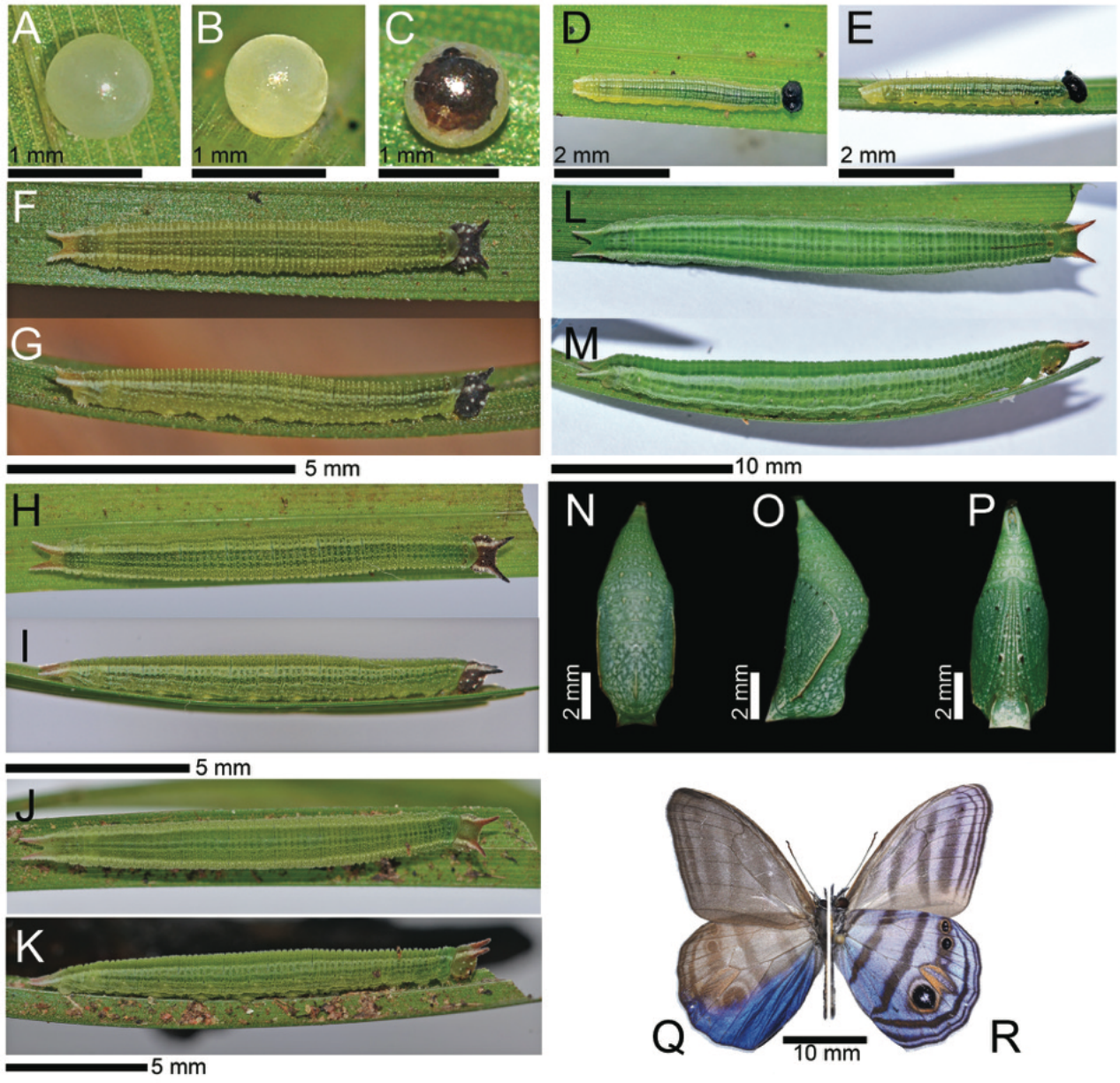

Figure 1. *Chloreuptychia chlorimene* life stages: (A, B) egg in dorsal and lateral view; (C) egg with the formed head capsule visible; (D, E) first instar in dorsal and lateral view; (F, G) second instar in dorsal and lateral view; (H, I) third instar in dorsal and lateral view; (J, K) fourth instar in dorsal and lateral view; (L, M) fifth (ultimate) instar in dorsal and lateral view; (N, O, P) pupa in dorsal, lateral, and ventral view; (Q, R) adult in dorsal and ventral view (photos A, B, F, G, L–P are of 2025-FLP-IMM-0064; photos C–E, H–K are of 2025-FLP-IMM-0065; photos Q, R are of 2025-FLP-IMM-0091).

granulations across body. Thin subspiracular turquoise line from A1 to A8. Bifid caudal filaments are pinkish. Close to pupal stage, body changes to lighter green color, decreases in size, and turquoise subdorsal line becomes fainter. Body length: 26.3–30.3 mm ($n = 2$). Duration: 9 days ($n = 2$).

Pupa (Figs. 1N, O, P). In most individuals, body light green with scattered irregular whitish spots and some black spots in legs and marginal regions of wing case. Posterior edge of wing case yellowish-cream. Subtriangular keel with yellowish cream edge in mesothorax. Body overall slender with whitish squared ocular caps. Cremaster subtriangular, light green, short and gradually narrowing toward distal end in posterior view, with slightly pitted sculptures and multiple brown hooked setae. Body length: 11.9–12.0 ($n = 3$). Duration: 8–10 days ($n = 4$).

Remarks. A total of 11 individuals were found feeding on *Scleria* sp, of which 10 emerged as adults. The life cycle spanned an average 43.5 days ($n = 4$) from egg to

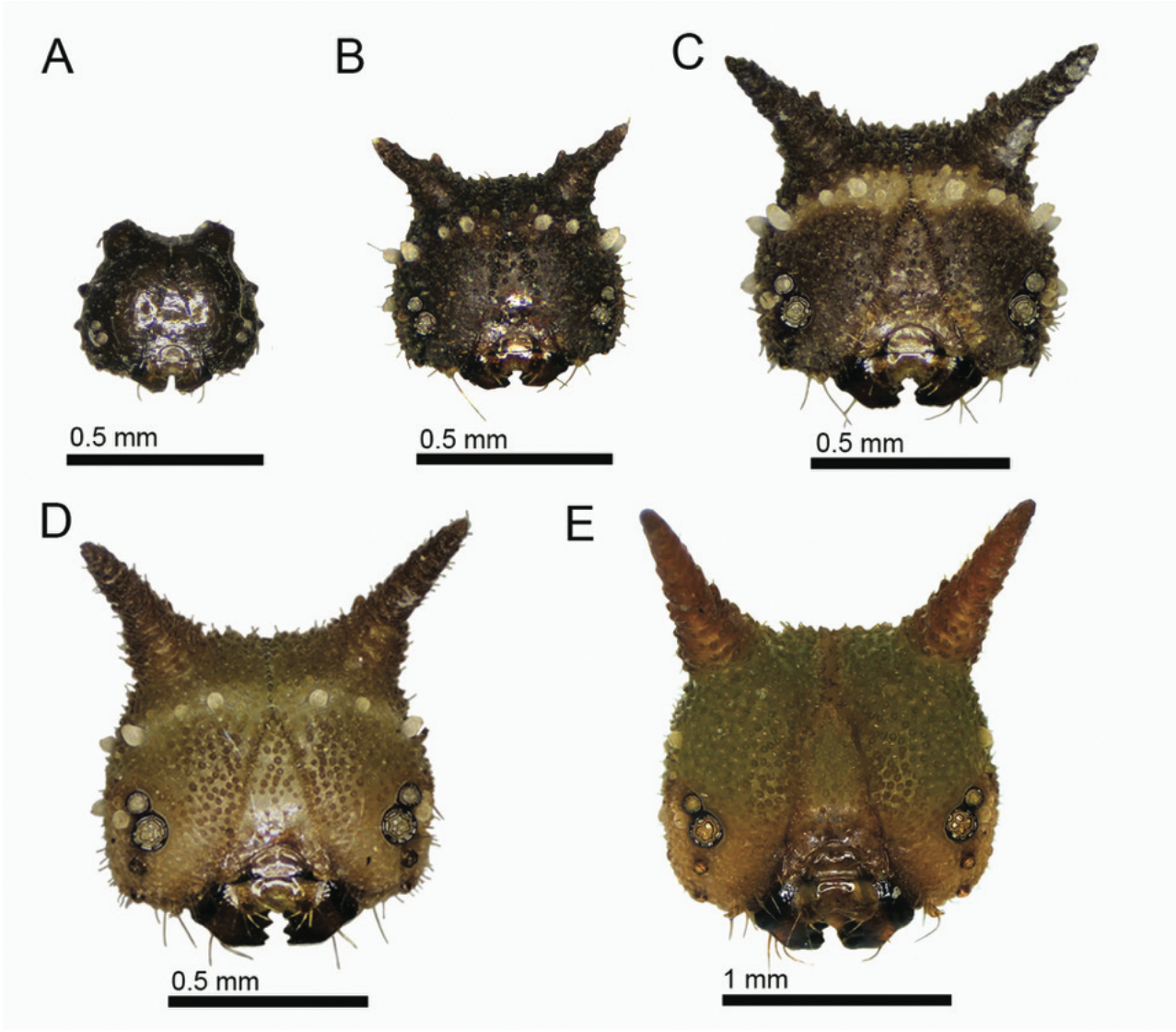

Figure 2. *Chloreuptychia chlorimene* larval head capsules collected and photographed after molting (all in front view): (A) first instar; (B) second instar; (C) third instar; (D) fourth instar; (E) fifth (ultimate) instar. (all photos are of 2025-FLP-IMM-0015).

adult emergence. The description we provide is based on the life cycle exhibiting five larval instars, as this is the most common condition among the reared individuals (Supplementary Table S2). Four additional individuals were found feeding on *Scleria secans*. Two of these records were collected in the antepenultimate instar, one in the first instar, and the remaining one was parasitized. Eight wasps, probably belonging to the genus *Cotesia* (Ichneumonoidea: Braconidae), emerged from the parasitized individual. The specimen collected in the first instar took 92 days to reach adulthood and passed through eight larval instars (2025-FLP-IMM -0105; Figure 3). Morphologically, and compared with the more common condition of five instar, this individual appears to have an extended third instar undergoing four molts, a fourth instar with two molts, and the absence of a fifth instar. All larvae were found primarily on the abaxial and distal regions of the leaf, where they were feeding near to obvious feeding damage.

Host plants

Scleria sp. (Cyperaceae: Cyperoideae: Sclerieae) (Figure 4)

The individuals of *Scleria* sp. grow at ground level and are most often found in forest sections with relatively high access to light, such as Cacao plantations. However, no individuals are observed in light gaps within the forest or open areas, and their abundance

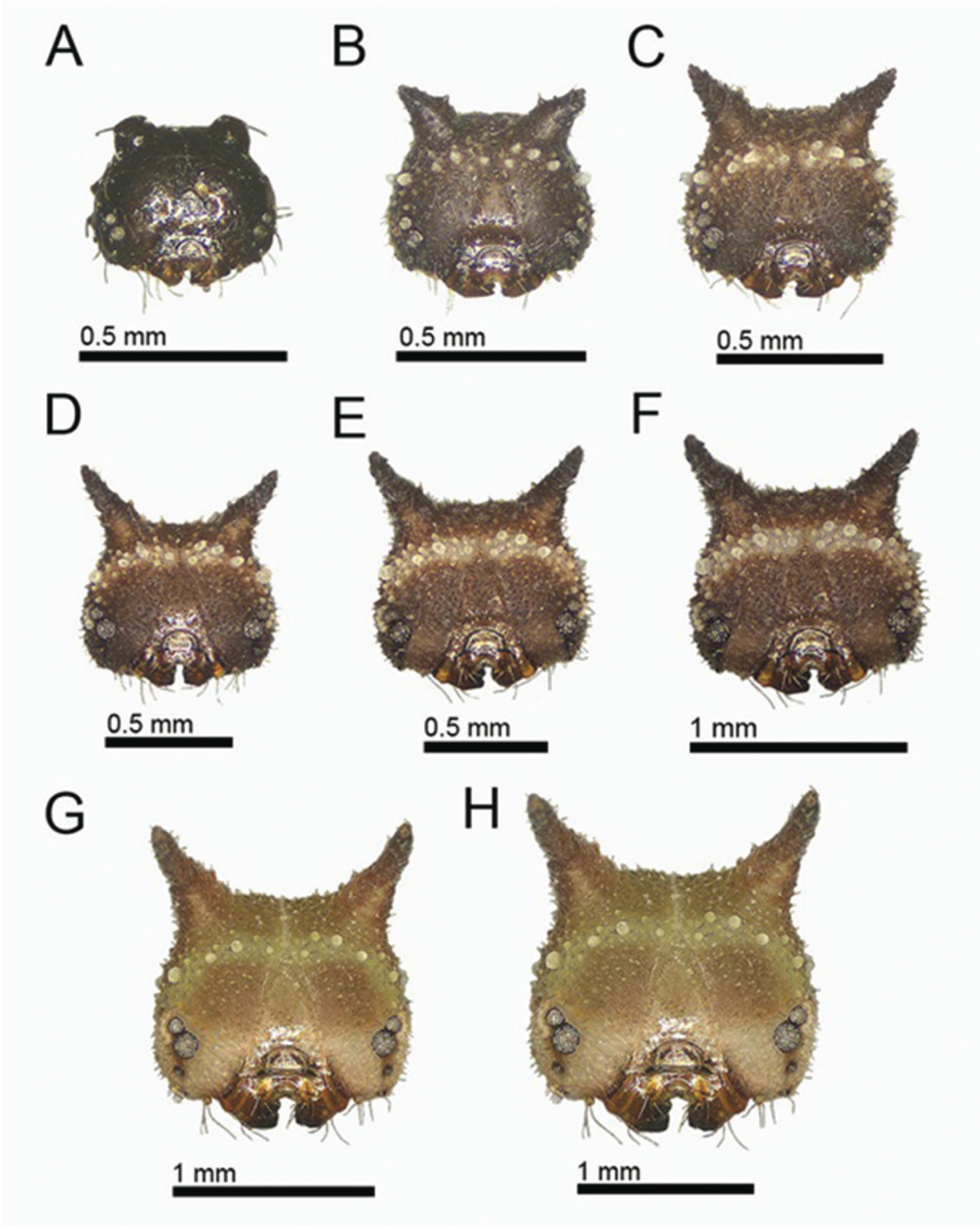

Figure 3. Head capsules of *Chloreuptychia chlorimene* reared on *Scleria secans* (all in frontal view): (A) first instar; (B) second instar; (C) third instar; (D) fourth instar; (E) fifth instar; (F) sixth instar; (G) seventh instar; (H) eighth (ultimate) instar (all photos are of 2025-FLP-IMM-0105).

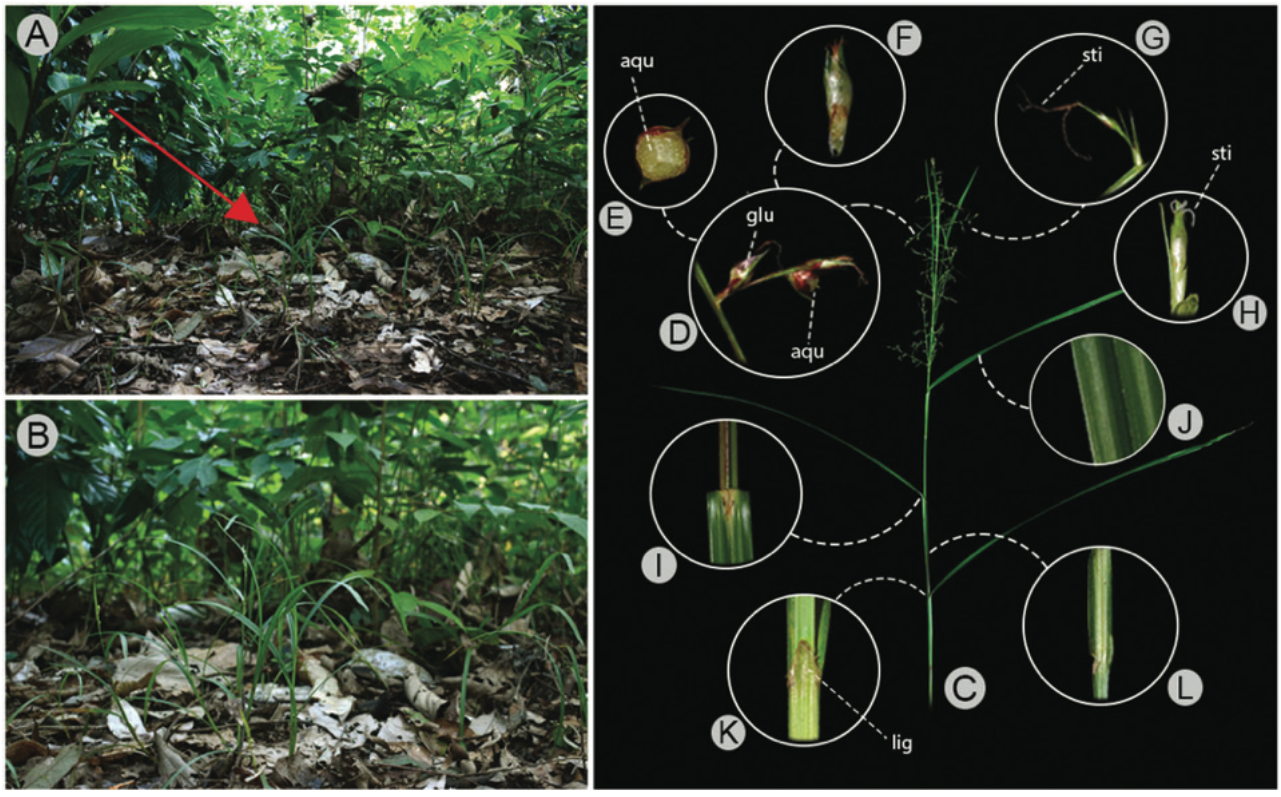

Figure 4. *Scleria* sp., hostplant for *Chloreuptychia chlorimene, Modica myncea*, and *Pierella hyalinus*: (A) plant in habitat; (B) *Scleria* sp in situ; (C) frontal view of the last segment of the stem and inflorescence; (D) position of the fruits; (E) dorsal view of the fruit; (F) side view of the flower; (G) position of the flower (sti: stigma); (H) flower (sti: stigma); (I) close-up of the base of the leaf; (J) close-up of the adaxial side of the leaf and serrated edge; (K) (lig: ligule); (L) winged stem.

decreases in areas with reduced light availability. The plants are small, reaching up to 30 cm in height. They are not strictly solitary, as they usually grow less than 1 m apart from each other, forming small groups, mainly in areas where the soil is little colonized by other herbs.

The host plant of the registered *C. chlorimene* individuals, as well as the leaves used for their feeding, are distributed at ground level within an agroforestry plot. This area is composed of cacao trees and forest species that exceed 3 m in height (e.g. *Ochroma pyramidale* (Cav. ex Lam.) Urb., *Cecropia peltata* L., *Aparisthmium cordatum* (A. Juss.) Baill.), which generate shade and allow a moderate entry of light.

Scleria secans (L.) Urb (Cyperaceae: Cyperoideae: Sclerieae) (Figure 5)

The individual of *S. secans* is a sedge (Cyperaceae) that grows solitarily both along the margins and within the interior of 'aguajales.' Seedlings do not exhibit an epiphytic habit until reaching approximately 1 m in height; thereafter, they begin to use the branches of other plants as support for their stem and branching. In larger individuals, the epiphytic habit becomes fully developed. Several stems were observed emerging from a single point at ground level; these stems are erect, thickened, and leafless until exceeding 1 m in height. Subsequently, they branch and spread widely over the branches and foliage of the supporting plants. The branches show predominantly vertical growth, although some develop horizontally, and others occur near ground level.

The host plant of *C. chlorimene* and *E. antonina* was found on the edge of a small stream that is within the 'aguajal.' The plant was epiphytic of a *Socratea* H. Karst palm and grew vertically along the stem axis of the palm. The maximum height was 3 m, but with some branches located near ground level.

Erichthodes antonina (C. Felder and R. Felder, 1867)

Vouchers. 2024-FLP-IMM-0704, 0736, 0765, 0786, 0790, 0794, 0795, 0796, 0799, 0800, 0815, 0816, 0817, 0818, 0819, 0820, 2025-FLP-IMM-0066, 0067, 0068, 0069, 0070, 0071a, 0071b, 0072, 0073, 0089, 0090,

0116, 0117, 0118, 0127, 0128 (GenBank vouchers: PZ007836, PZ007837, PZ007838, PZ007839).

Egg (Figure 6A, B). Spherical; bright whitish, slightly cream before hatching; chorion surface with irregular pitted sculpting; head capsule and body setae visible one day prior to hatching. Diameter: 0.95–0.97 mm ($n = 3$). Duration: Unknown, hatched 3–4 days after collection.

First instar (Figure 6C, D, E, F). Head capsule width 0.54 mm ($n = 2$). Head capsule brown (Figure 7A), darkening near mandibular and ecdysial areas; shiny, with multiple surface striations. Two short subrectangular scoli, slightly bifurcated apically (scolus length 0.10 mm, $n = 1$), each bearing two broad brown setae, one at each end. Four chalazae visible in frontal view (M1, M2, M3, P4), all terminating in thick brown setae. Labrum with five setae visible on one side. Six stemmata present; stemmata 2 and 3 slightly larger, stemma 3 largest and closer to stemma 2 than to 4; stemmata 1 and 6 semi-transparent and poorly defined. Body integument creamy whitish, semi-transparent; dark green from T1 to A8 and yellowish in posterior segments after feeding. Tracheal system yellowish. Short, thick brown setae distributed over body, slightly longer from A8 to A10. Caudal filaments short, slightly yellow, bifid, each ending in a long, thick brown seta. Body length 3.0–6.0 mm. Duration: 9 days ($n = 2$).

Second instar (Figure 6G, H). Head capsule width 0.74–0.76 mm ($n = 2$). Head capsule dark brown (Figure 7B) with pitted sculpturing; epicranial marking slightly darker. Multiple short secondary setae and scattered protuberances present. Two well-developed bifurcating scoli (scolus length 0.15 mm and 0.23–0.25 mm including bifurcations; $n = 2$), divided in distal third, each branch bearing thick, short black setae apically; scoli bases with multiple protuberances. Three whitish dorsal chalazae (M1, M2, M3), each ending in a brown seta. Six stemmata visible, similar to immediately preceding instar. Lower frons and adjacent lateral areas paler. Creamy band with short protuberances between M1 chalazae, extending posteriorly near SS1–SS3 setae. Creamy thin posterior stripe extending from scoli bases to base of head capsule, with short scattered protuberances; extent and intensity variable among individuals. Body granular, with multiple yellowish tubercles, more abundant dorsolaterally. Body dark green from T1 to A8; green mid-dorsal line from T1 to A6, becoming pinkish from A7 to A10. Subdorsal pinkish stripe from A7 to A10; small pinkish patches scattered on A8–A10. Pale yellow stripe in subdorsal and subspiracular regions. Caudal filaments short, bifid, pinkish on inner side and whitish dorsally, bearing short black setae. Body length 6.0–10.0 mm. Duration 15 days ($n = 2$).

Third instar (Figure 6I, J). Head capsule width 1.0–1.15 mm ($n = 3$). Head capsule (Figure 7C) translucent green immediately after molting, dark brown as instar progresses. Shape and color pattern similar to immediately preceding instar, but creamy bands more distinct and paler. Scoli larger (scolus length 0.50–0.55 mm, including bifurcations; $n = 2$), slightly green posteriorly near T1; scoli bases with creamy dorsal protuberances. Body similar to immediately preceding instar, a thin subdorsal yellow stripe. Bifid, longer, pinkish caudal filaments changing to slightly turquoise shortly before molting. Body length: 15.5–18.5 mm ($n = 1$). Duration: 14 days ($n = 1$).

Fourth instar (Figure 6K, L). Head capsule width: 1.4 mm ($n = 1$). Head capsule similar to immediately preceding instar (Figure 7D), but with more conspicuous dorsal protuberances at scoli bases and more evident green spots on posterior side; scoli larger. Body yellow immediately after molt, turning green with multiple brownish spots from T1 to A4 and A6 to A10. Mid-dorsal line diffuse yellowish, becoming pinkish from A8 onward. Thick dorsolateral yellow stripe from T1 to A10. Caudal filaments bifid, pinkish internally and turquoise externally and dorsally, the base of the setae of the inner end are black. Body length: 15.5–18.5 mm ($n = 1$). Duration: 11–20 days ($n = 3$).

Five instar (Figure 6M, N). Head capsule width: 1.74 mm ($n = 1$). Head capsule similar to immediately preceding instar (Figure 7E); bands and spots cream-yellowish. Upper frons slightly green; creamy lower frontal band and adjacent lateral area extending to stemmata 3 and 4. Lateral green line present; two vertical green lines with yellow margins on posterior side. Epicranial suture yellow; some yellow spots posterior to stemmata. Scoli dark brown laterally, gradually becoming light cream from mid-length to base, larger than in previous instar (scolus length: 1.15 mm including bifurcations; $n = 1$). Body light green with yellow-green micro-granulation dorsally and laterally. Gray mid-dorsal line from T1 to T3, widened at T1, followed by light green triple-width line from A1 to A10. Yellowish-green subdorsal band with a distinct fine white line above, formed by micro-granulations. Granulations elongated in dorsolateral region. Diffuse yellowish-green line in spiracular region. Spiracles creamy orange with brown margins. Caudal filaments dark green overall, apex and extension of dorsolateral line turquoise, with scattered black tubercles apically, ventrally and between the caudal filaments. Body length: 28–38 mm ($n = 3$). Duration: 20 days ($n = 1$).

Pupa (Figure 6O, P, Q; Figure 8C, D). Body overall yellowish green, mottled with white; abdominal dorsum darker, appearing semi-rectangular in lateral view. Ocular caps green with posterior brown spots. Mesothorax strongly elevated, with brown mid-dorsal spot, thickened near prothorax and bifurcated near metathorax. Abdomen with paired white-yellowish dorsal lines formed by discontinuous spots. Wing case green with faint white venation; distal margin with cream-brown patch. Spiracles pale creamy brown from A2 to A8; creamy subspiracular line present. Ventrally, head margin white with brown edge; forelegs with two light brown medial points. One day before emergence, pupa entirely brown. Cremaster reddish brown with pitted sculpturing; creamy yellow lateral spot followed ventrally by a pink band. Body length: 9.8–8.0 mm ($n = 2$). Duration: 11–13 days ($n = 2$).

Remarks. A total of 32 individuals were found feeding on *Scleria secans*, of which six emerged as adults (Supplementary Table S2). The total duration of the life cycle is unknown, as we were unable to obtain the complete life cycle for a single specimen. However, the morphology of the head capsules indicates that we documented all larval instars of the species by examining different individuals at different developmental stages, and we estimate between 67 and 100 days to complete the life cycle. The larvae are highly sedentary, moving only a few centimeters per day. In the clutches of two individuals, the larvae remained together, separating only when feeding. In all instars, they rest on distal in the abaxial side of the leaf, near to obvious feeding damage.

Host plant. *Scleria secans* (L.) Urb. (Cyperaceae: Cyperoideae: Sclerieae) (Figure 5)

Modica myncea (Cramer, 1780)

Vouchers. 2025-FLP-IMM-0006, 0031, 0088 (GenBank voucher: PZ007832).

Egg (Figure 9A, B, C, D). Subelliptical, yellowish, shiny and smooth. Head capsule and body setae visible one day prior to hatching. Diameter: 0.67 mm ($n = 1$); height: 0.48 mm ($n = 1$). Duration: Unknown, hatched 4 days after collection ($n = 1$).

First instar (Figure 9E, F, G). Head capsule width: 0.42 mm ($n = 1$). Head capsule black (Figure 10A), shiny; two short subrectangular scoli (scolus length: 0.10 mm; $n = 1$), each with two broad setae, one at each end. Chalazae not visible. Labrum with five setae visible on one side. Six stemmata present; stemma 3 largest and closer to stemma 2 than to 4; stemmata 1, 5, and 6 paler and semi-translucent. Body integument semi-translucent, dark green after feeding from T1 to A5, yellowish from A5 to A10. Pair of whitish subdorsal stripes present. Semi-translucent globose setae distributed along body, larger on A8–A10. Caudal filaments short, bifid, barely discernible. Body length: 3.60 mm. Duration: 4 days ($n = 1$).

Second instar (Figure 9H, I). Head capsule width: 0.56–0.58 mm ($n = 3$). Head capsule matt-black (Figure 10B), with granular texture and pitted sculpting. Scoli well-developed, horn-like, with multiple protuberances (scolus length: 0.22 mm; $n = 1$). Chalazae not visible. Body light green with micro-granulations throughout. Slightly darker mid-dorsal line, turning reddish-brown on the last segments. Mid-dorsal line slightly darker, turning reddish brown on posterior segments. Thin, whitish, slightly sinuous subdorsal line present. Reddish-brown spots scattered in supra-spiracular region from A3 to A8. Caudal filaments bifid, pinkish, more conspicuous than in previous instar. Body length: 4.71 mm ($n = 1$). Duration: 4 days ($n = 1$).

Third instar (Figure 9J, K). Head capsule width: 0.74–0.78 mm ($n = 2$). Head capsule dark brown (Figure 10C) with scattered irregular paler spots. Scoli similar to immediately preceding instar (scolus length: 0.35 mm; $n = 1$), with pinkish apices and a broad creamy stripe on the posterior side extending onto the posterior head capsule; several protuberances on posterior and lateral surfaces. Body similar in shape and coloration to previous instar; tubercles whitish; pair of conspicuous whitish tubercles on each side of mid-dorsal line. Reddish-brown discontinuous sinuous line in supraspiracular region. Caudal filaments bifid, pinkish, approximately as long as A8. Body length: 10.3 mm ($n = 1$). Duration: 5 days ($n = 1$).

Fourth instar (Figure 9L, M). Head capsule width: 1.06 mm ($n = 3$). Head capsule light brown (Figure 10D) with numerous protuberances, especially on dorsal and posterior surfaces; darker protuberances irregularly distributed; pitted sculpturing and several secondary setae present. Dark brown band between scoli extending laterally to stemma 2. Scoli similar to previous instar (scolus length: 0.50–0.60 mm; $n = 2$), dark brown in frontal view, posteriorly pinkish with slight orange tint extending to mid-length. Creamy posterior band present but less conspicuous than in immediately preceding instar. Body light green; paired whitish tubercles on each side of mid-dorsal line from T1 to A8; numerous minute yellowish tubercles over entire body. Mid-dorsal line faint from T1 to A6, becoming reddish brown and more distinct from A7 onward. Supraspiracular line more discontinuous than in previous instar, with scattered minute whitish

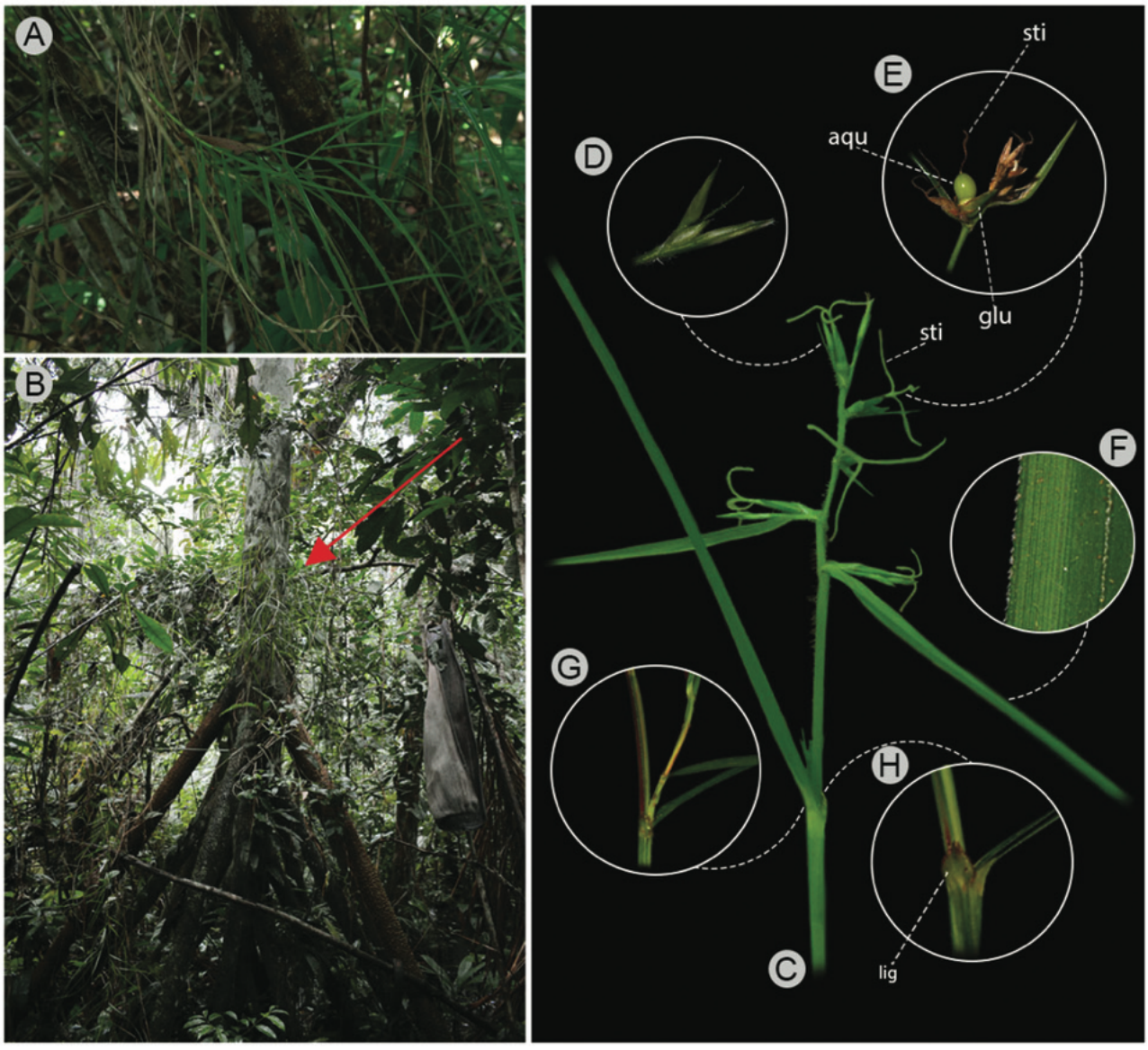

Figure 5. *Scleria secans*, hostplant for *Erichthodes antonina* and *Chloreuptychia chlorimene*: (A) *S. secans* in situ; (B) plant in habitat; (C) frontal view of the last segment of the stem and inflorescence (sti: stigma); (D) position of the fruit; (E) fruit (ach: achene, glu: glume, sti: stigma); (F) close-up of the abaxial side of the blade and notched edge; (G) frontal view of the branching; (H) close-up of the node (lig: ligule).

tubercles. Spiracles dark brown. Subspiracular region with irregularly distributed minute whitish tubercles; tracheal system whitish. Caudal filaments bifid, pinkish, slightly longer than A8, outer surface yellowish. Body length: 17.3 mm ($n = 1$). Duration: 7 days ($n = 1$).

Fifth instar (Figure 9N, O). Head capsule width: 1.58–1.64 mm ($n = 2$). Head capsule light brown (Figure 10E) at beginning of instar, with dark brown protuberances; becoming dark brown with rough surface as instar progresses. Scoli well-developed, horn-like, with expanded bases giving a robust appearance (scolus length: 0.75 mm; $n = 2$), apically pinkish in frontal view. Creamy band on posterior side of scoli extending onto posterior head capsule; brown band on inner side of scoli joining at notch. Body light brown with green spots near mid-dorsal line and subdorsal region, turning dark brown as instar progresses, with darker mid-dorsal line from T1 to T3. Several micro-granulations distributed over body, largest whitish micro-granulations arranged in subdorsal, supraspiracular, and subspiracular lines. Subdorsal zigzag line well defined; supraspiracular zigzag line weaker. Spiracles black. Caudal filaments bifid, dark brown, with paler outer surface. Body length: 25.6 mm ($n = 1$). Duration: 8–10 days ($n = 2$).

Pupa (Figure 9Q, R). Body black mottled with grayish-creamy spots. Body short, rounded, with squared

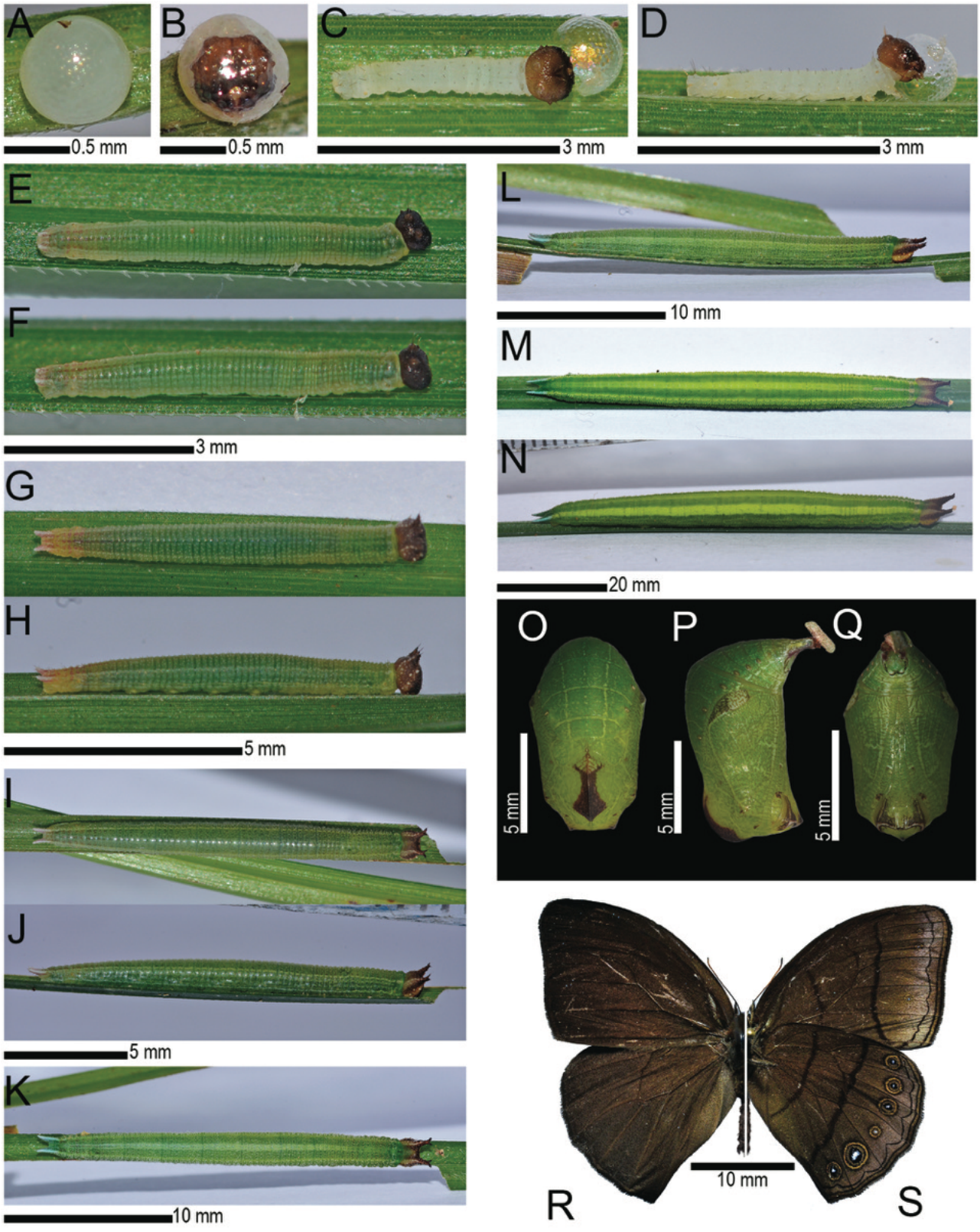

Figure 6. *Erichthodes antonina* life stages: (A) egg in dorsal view; (B) egg with formed head capsule; (C, D) newly hatched larva feeding on the chorion, in dorsal and lateral view; (E, F) first instar in dorsal and lateral view; (G, H) second instar in dorsal and lateral view; (I, J) third instar in dorsal and lateral view; (K, L) fourth instar in dorsal and lateral view; (M, N) fifth (ultimate) instar in dorsal and lateral view; (O, P, Q) pupa in dorsal, lateral and ventral view; (R, S) adult in dorsal and ventral view (photos A, B are of 2024-FLP-IMM-0794; photos C, D are of 2024-FLP-IMM-0795; photos E–L are of 2024-FLP-IMM-0817; photos M–O are of 2024-FLP-IMM-0765; photos O–Q are of 2024-FLP-IMM-0704; photo of the adult does not correspond to that of the emerged adult).

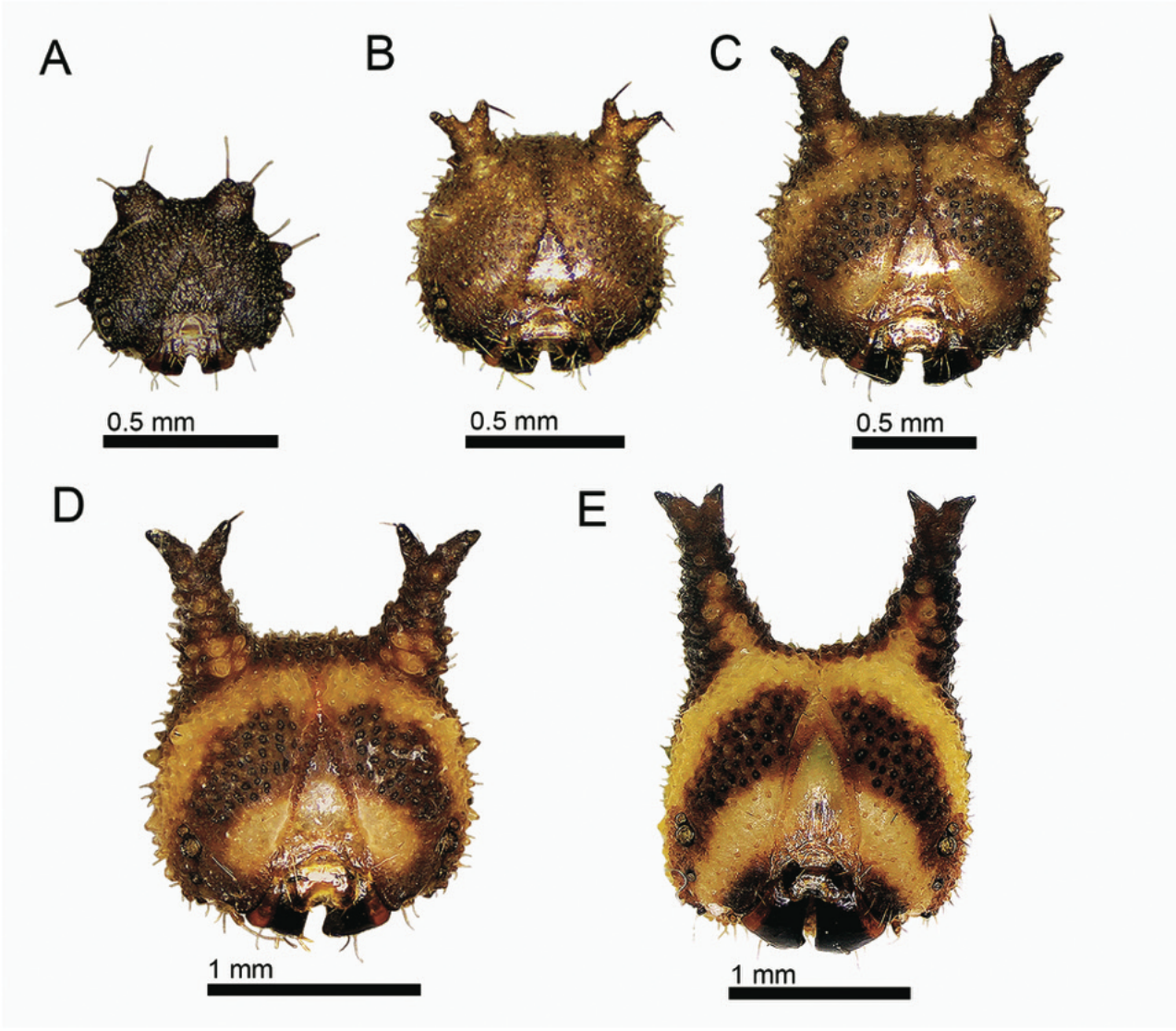

Figure 7. *Erichthodes antonina* larval head capsules collected and photographed after molting (all in frontal view): (A) first instar; (B) second instar; (C) third instar; (D) fourth instar; (E) fifth (ultimate) instar (photos A–D are of 2024-FLP-IMM-0817; photo E is 2024-FLP-IMM-0704).

ocular caps. Spiracles dark brown. Mesothorax prominently elevated. Abdomen dorsally with two rows of black protuberances bearing pinkish tips. Cremaster black, rectangular in lateral view, with light brown pitted sculpturing. Body length: 10.1 mm ($n = 1$). Duration: 9–10 days ($n = 2$).

Remarks: A total of three individuals were found feeding on *Scleria* sp, of which all emerged as adults. The life cycle spanned 35 days ($n = 1$) from egg to adult emergence (Supplementary Table S2). Proportionally, this species was less frequently encountered than *C. chlorimene*. The larva was usually located on the abaxial and distal part of the leaf, where it fed, near to obvious feeding damage. When threatened, it would rapidly move the anterior part of its body from side to side.

Host plant. *Scleria* sp (Cyperaceae: Cyperoideae: Sclerieae) (Figure 4)

Magneuptychia libye (L.)

Voucher. 2025-FLP-IMM-0003.

Egg to pupa. Larval head capsules documented (Figure 11), otherwise immature stages not detailed. See Kaminski and Freitas (2008) for a full description of the immature stages.

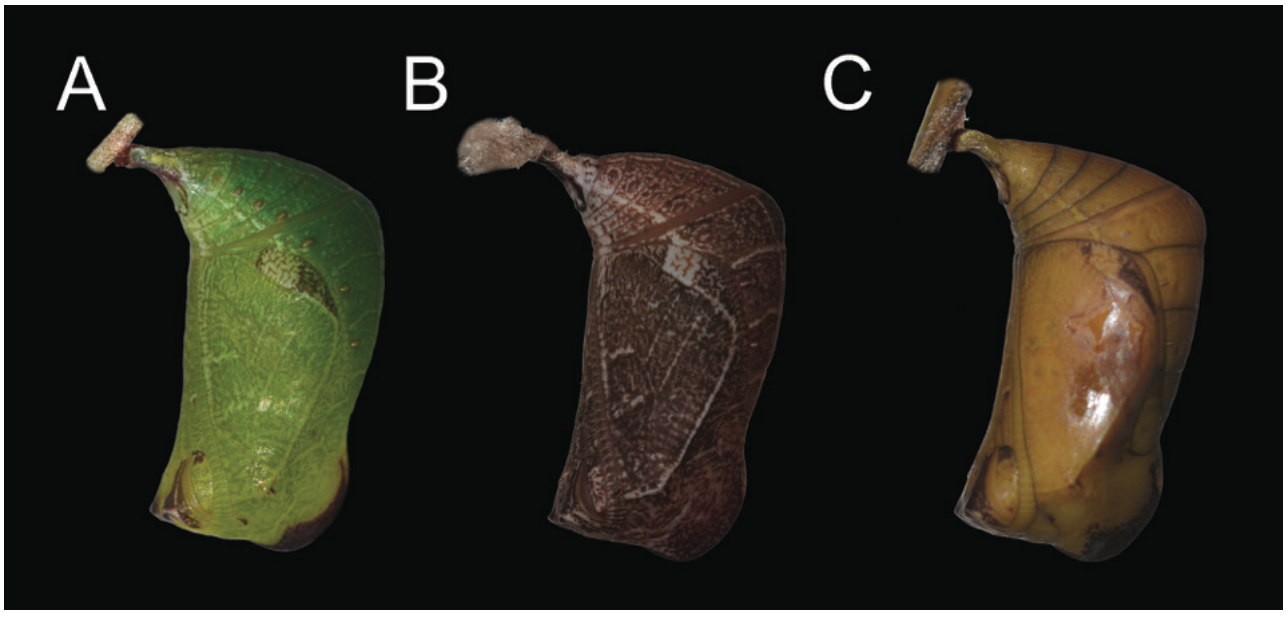

Figure 8. Pupal coloration in *Erichthodes antonina*: (A) green morph (2024-FLP-IMM-0704); (B) brown morph (2025-FLP-IMM-0066); (C) parasitized pupa (2025-FLP-IMM-0067).

Host plant. *Scleria* sp. (Cyperaceae: Cyperoideae: Sclerieae) (Figure 4)

Pierella hyalinus (Gmelin, [1790])

Voucher. 2025-FLP-IMM-0004.

Antepenultimate instar (Figure 12A, B). Head capsule width: 1.08 mm ($n = 1$). Frontal view of head capsule black with three reddish spots (Figure 13A): one near the intersection of the epicranial suture and the lateral adfrontal suture, and the other two near the base of the frontoclypeus, one on each side. Lateral and posterior side of head capsule brown and bumpy. Head capsule with multiple translucent setae. Scoli very short, unbranched, and triangular (scolus length: 0.15 mm; $n = 1$). Mottled brown body with reddish tones. Tiny whitish tubercle in body. White spots in subdorsal region from T2 to A6. Black spiracles. Light brown tracheal system. Brown bifid caudal filaments with tip lighter. Body length: 18.4 mm ($n = 1$). Duration: unknown, molted 4 days after sampling ($n = 1$).

Penultimate instar (Figure 12C, D). Head capsule width: 1.65 mm ($n = 1$). Head capsule similar to previous instar (Figure 13B), but lateral protuberances larger and creamy, scoli more rounded (scolus length: 0.20 mm; $n = 1$). Body similar to previous instar, but with a diffuse black subdorsal line from T2 to A6. Caudal filaments more evident, almost twice as long as A8. Body length: 28.8 mm ($n = 1$). Duration: 9 days ($n = 1$).

Ultimate instar (Figure 12E, F). Head capsule width: 2.2 mm. Head capsule similar to previous instar (Figure 13C), with reddish spots near the intersection of the epicranial suture and the lateral adfrontal suture more clearly defined, with a triangular arch shape, a brown-reddish lateral spot near to stemmata 4. Body darker brown than in the previous instar, with a zigzag subdorsal line, with groups of white tubercles regularly spaced. A smaller group of tubercles in the supraspiracular region. Bifid caudal filaments with a group of cream-whitish tubercles at the base. Body length: 38.3 mm. Duration: 20 days ($n = 1$).

Pupa (Figure 12H, I, J). Body dark brown mottled with light brown. Wing case light brown with dark brown spot in distal area of discal cell. Squared ocular caps, with creamy tips. Forewing case with white spots. White spots in two rows on the abdomen in dorsal view. Dark brown cremaster, appearing rectangular in lateral view, with light brown hooked setae. Body length: 17.8 mm. Duration: 14 days ($n = 1$).

Remarks. Only one individual was found on *Scleria* sp., resting on a dry stem near a plant that showed leaf damage. The larva likely corresponds to the second instar. In all instars, the larva was located at the base of the leaves or on stems facing the ground, far from where the larva was feeding. This may reflect its natural behavior of positioning itself on the host plant's stems for camouflage. The larva preferentially fed at night, subsequently returning to its position on the plant stem. When threatened, the larva would drop from the stem and remain motionless for several minutes.

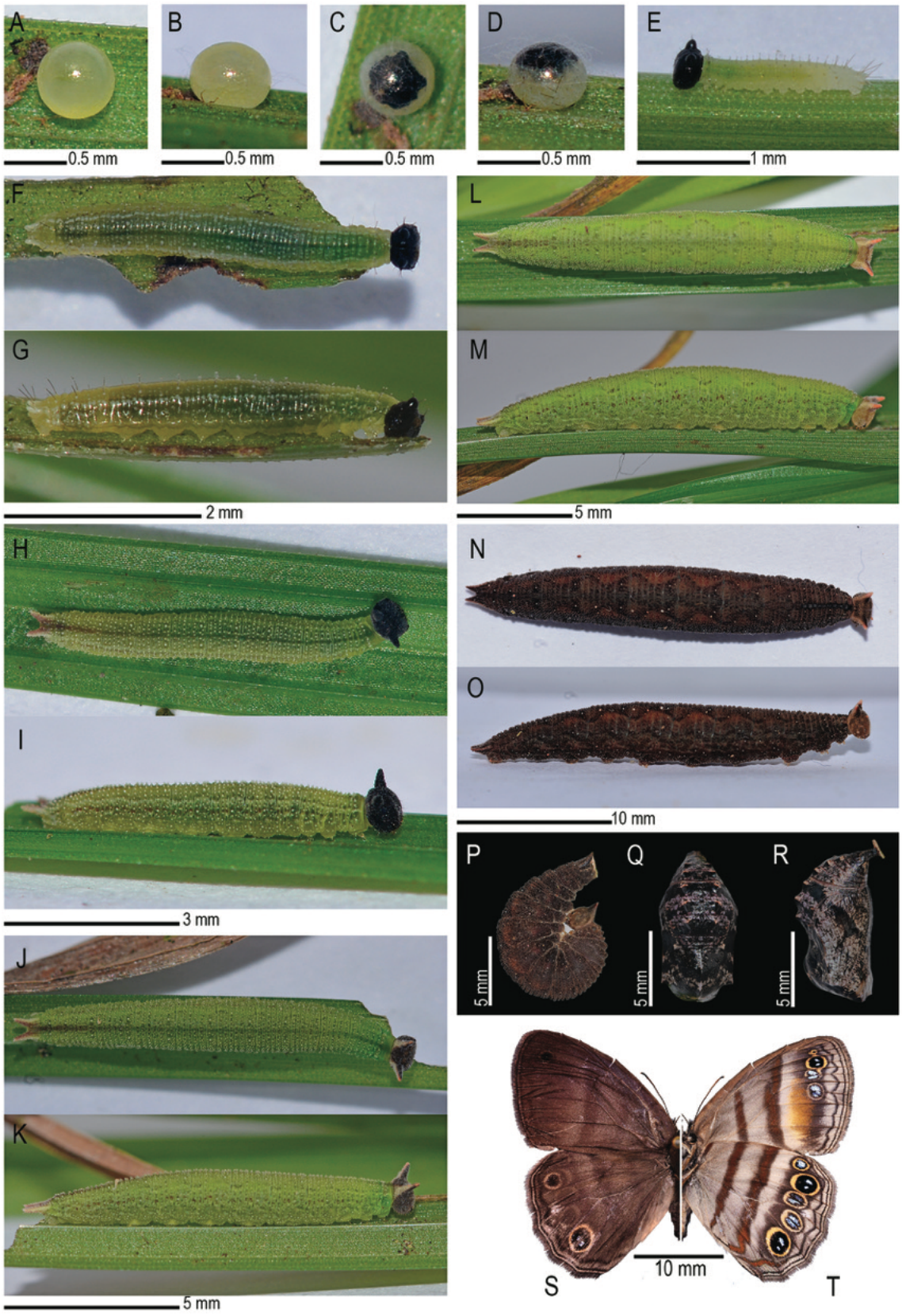

Figure 9. *Modica myncea* life stages: (A, B) egg in dorsal and lateral view; (C, D) egg with the formed head capsule, in dorsal and lateral view; (E) newly hatched larva; (F, G) first instar in dorsal and lateral view; (H, I) second instar in dorsal and lateral view; (J, K) third instar in dorsal and lateral view; (L, M) fourth instar in dorsal and lateral view; (N, O) fifth (ultimate) instar in dorsal and lateral view; (P) prepupa in lateral view; (Q, R) pupa in dorsal, and lateral view; (S, T) adult in dorsal and ventral view (all photos are of 2025-FLP-IMM-0006).

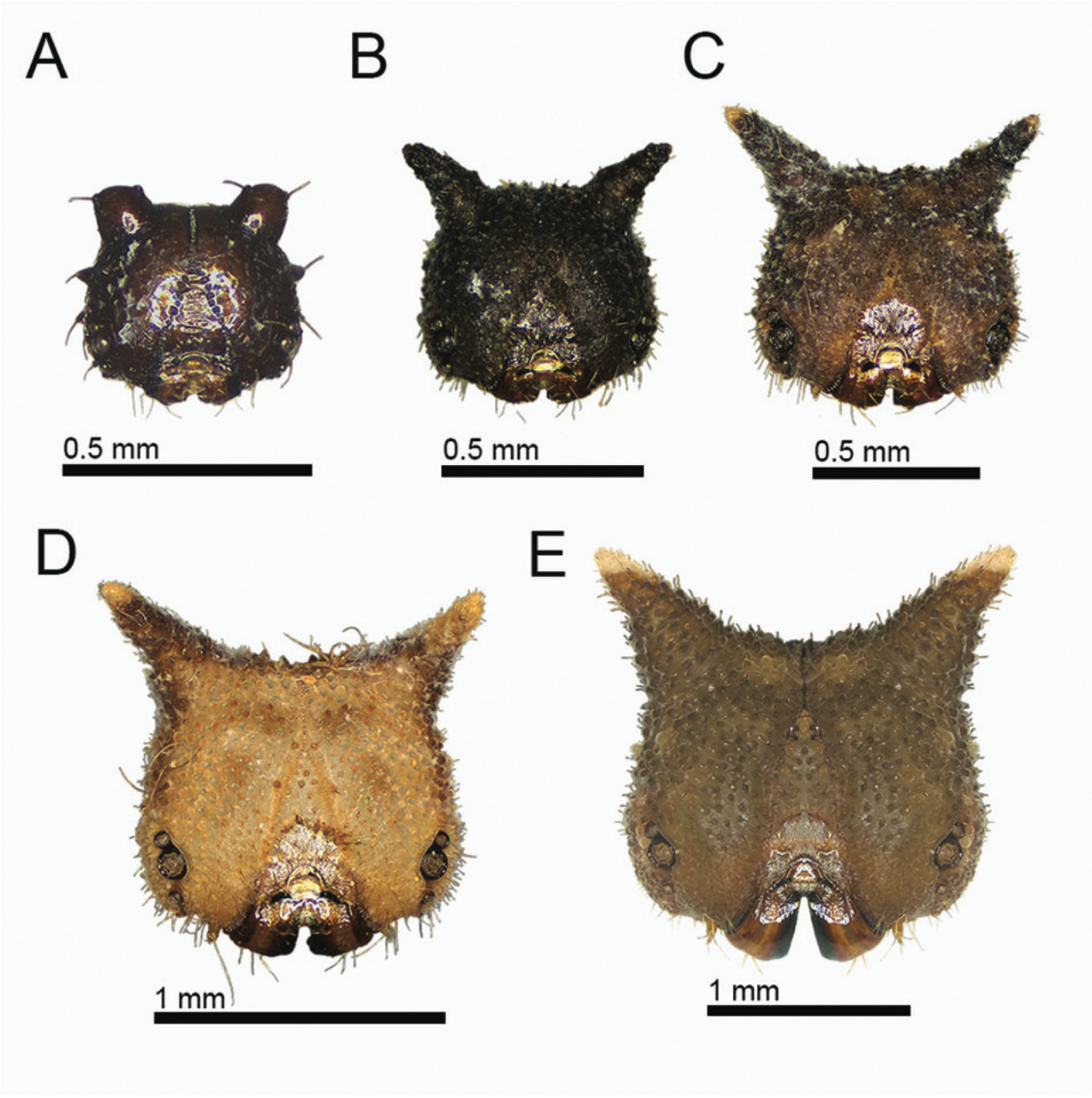

Figure 10. *Modica myncea* larval head capsules collected and photographed after molting (all in frontal view): (A) first instar; (B) second instar; (C) third instar; (D) fourth instar; (E) fifth (ultimate) instar (photos A–D are of 2025-FLP-IMM-0006, photo E is 2025-FLP-IMM-0031).

Host plant: *Scleria* sp. (Cyperaceae: Cyperoideae: Sclerieae) (Figure 4)

Discussion

The satyr species documented in this study belong to multiple genera across two tribes and exhibit markedly distinct morphological characteristics; they also share similar adaptations and behaviors that render them inconspicuous. Below, we discuss our detailed findings in three sections, mentioning the features shared by species where applicable, the possible phylogenetic implications of these shared characters, and aspects shared by all studied species potentially related to their use of Cyperaceae as host plants.

Comparative morphology of immature stages

Across all larval stages, larvae of *C. chlorimene* exhibit a broad longitudinal subdorsal band, which becomes whitish in the final instar, resembling the pattern

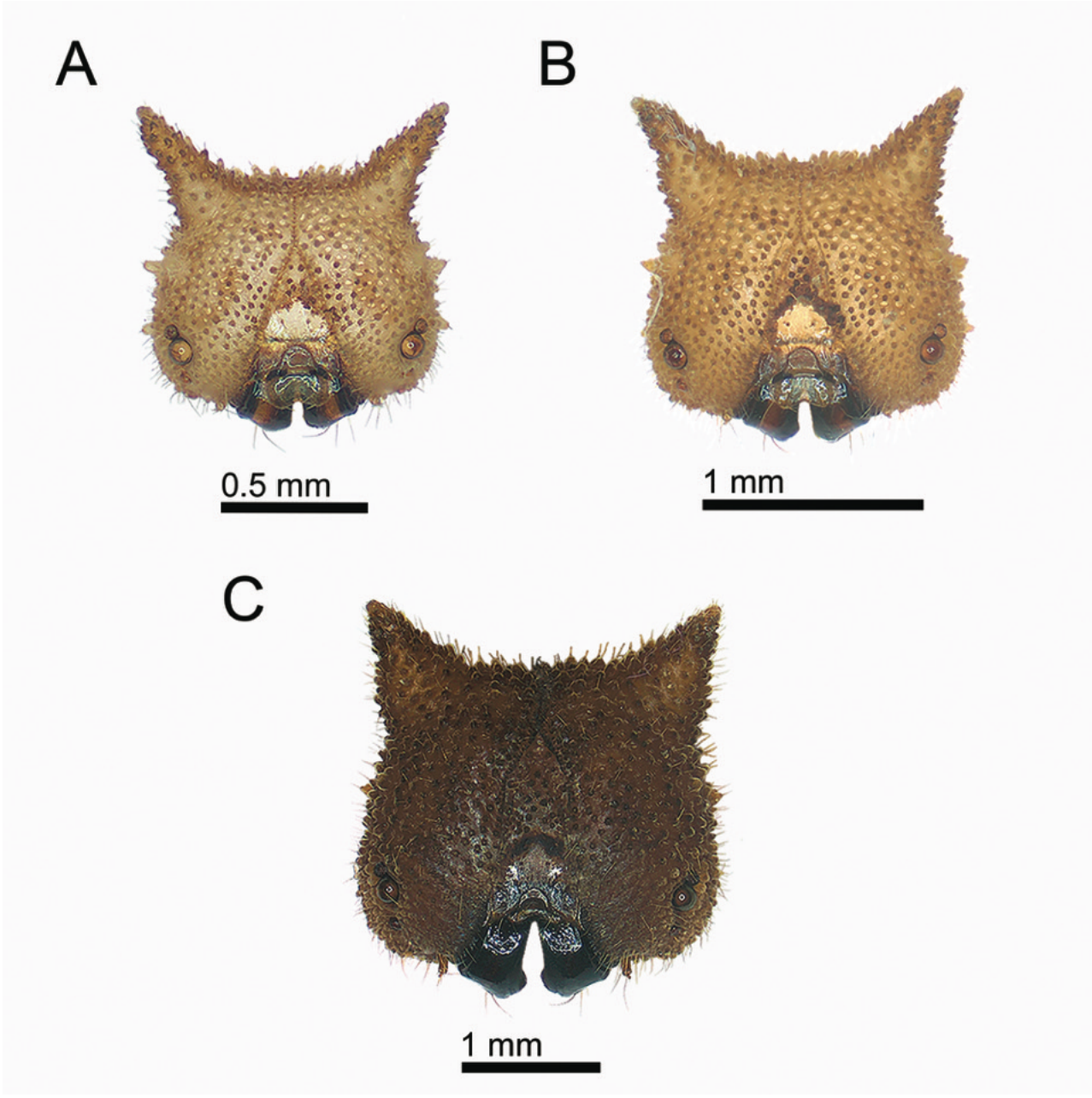

Figure 11. *Magneuptychia libye* larval head capsules collected and photographed after molting (all in frontal view): (A) third instar; (B) fourth instar; (C) fifth (ultimate) instar (all photos are of 2025-FLP-IMM-0003).

observed from the second to fourth instars of *Nhambikuara furina* (Hewitson, 1862) and *N. mima* (Butler, 1867) (Corahua-Espinoza et al. 2022b). Whitish longitudinal bands have also been recorded in other Euptychiina species (e.g. Freitas 2003; Freitas et al. 2016; Willmott et al. 2019), and even in Pronophilina (e.g. Greeney et al. 2010; Montero and Ortiz 2012; Padrón et al. 2019), although in these groups they tend to be thinner and may disappear in the final instar. Remarkably, a similarly broad subdorsal band was also observed in the last instar of *E. antonina*, although yellow-green in color, as well as in another Pyralidae species feeding on *Scleria* sp. (Figure 14).

The pupa of *C. chlorimene* typically exhibits a green coloration mottled with white, with a whitish band encircling the posterior margin (Figure 1N-P). This trait has also been reported in other Euptychiina species associated with various Poaceae, particularly bamboos, including *Satyrotaygetis iris* (Corahua-Espinoza et al. 2022a), *Taydebis melobosis* (Capronnier, 1874) (as '*T. peculiaris*') (Freitas 2003), several species of *Taygetis* (Young 1984, Freitas 2017; Hurtado et al. 2021), and *Optimandes eugenia* (Willmott et al. 2019). It is

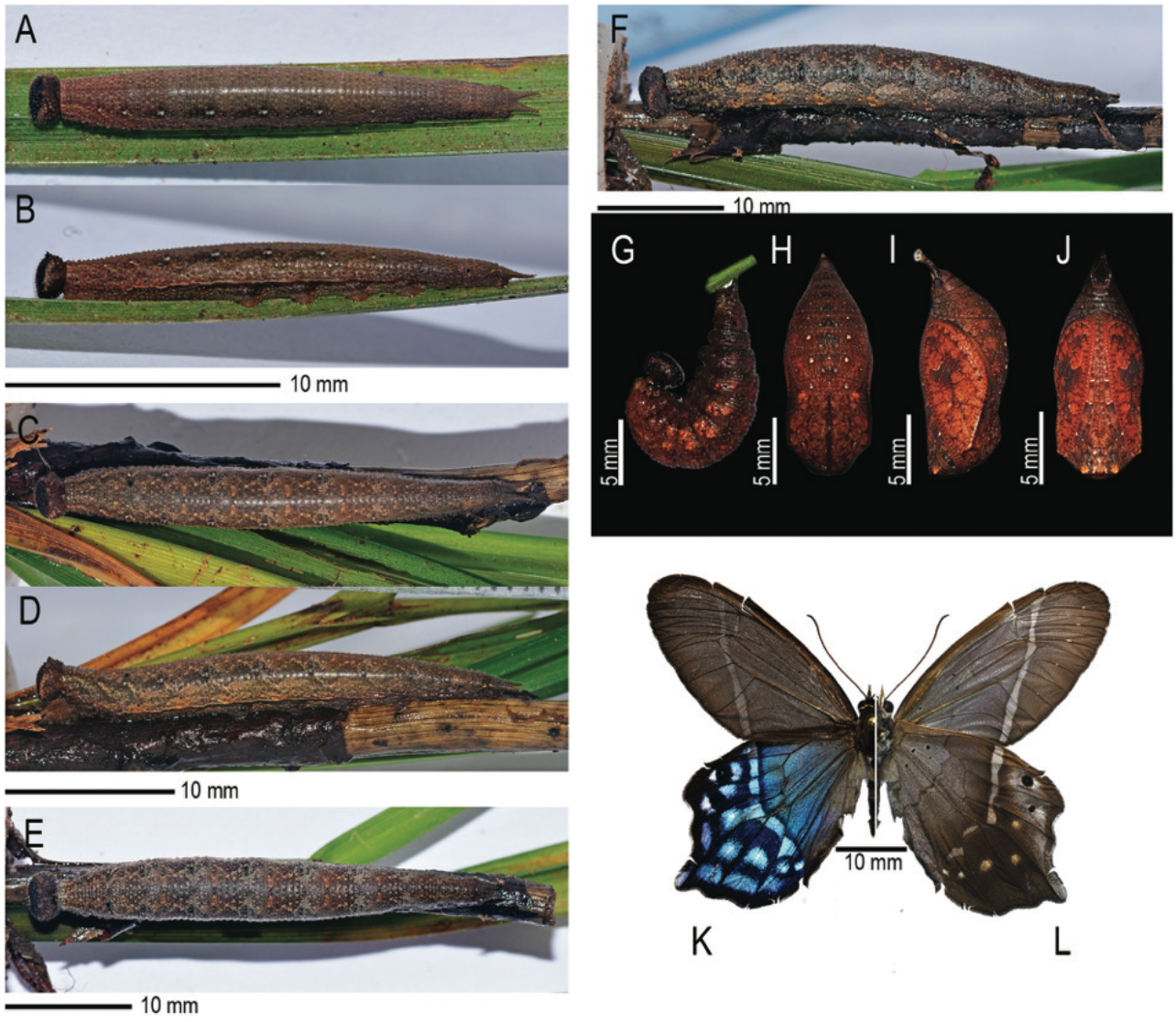

Figure 12. *Pierella hyalinus* life stages: (A, B) antepenultimate instar in dorsal and lateral view; (C, D) penultimate instar in dorsal and lateral view; (E, F) ultimate instar in dorsal and lateral view; (G) prepupa in lateral view; (H, I, J) pupa in dorsal, lateral and ventral view; (K, L) adult in dorsal and ventral view (all photos are of 2025-FLP-IMM-0004).

likewise shared with species belonging to Pronophilina, such as *Lymanopoda* spp. Westwood, 1851 (Montero and Ortiz 2012; Padrón et al. 2019), *Junea dorinda* (C. Felder and R. Felder, 1862) (Montero and Ortiz 2012), and species of *Corades* Doubleday, [1849] (e.g. Greeney et al. 2010; Montero and Ortiz 2014).

Chloreuptychia chlorimene also exhibits striking differences in comparison with other species groups, particularly in pupal shape and ornamentation. While pupae from the '*Pareuptychia* clade' and '*Archeuptychia* clade' (as defined by Espeland et al. 2023) are typically short with rounded ocular caps, pupae of *C. chlorimene* are noticeably more elongated and slender, with square or triangular ocular caps, resembling those of *Amiga arnaca* (Fabricius, 1776) (DeVries 1987) or *Nhambikuara* Freitas, Barbosa and Zacca, 2018 (Corahua-Espinoza et al. 2022b; Freitas 2022). In addition, the length, thickness, and orientation of the scoli in *C. chlorimene* are distinctive, more similar to the horn-like scoli of *Pseudeuptychia marica* (Weymer, 1911) (Tejeira et al. 2021), although in this case bright orange-reddish in color. This contrasts with the short, branched, or smaller and pointed horn-like scoli present in other clades.

As in other species of the '*Pareuptychia* clade,' the immature stages of *E. antonina* exhibit distally branched scoli, an elongate body with micro-granulations and pale longitudinal bands, green coloration with a broad, paler subdorsal band, short bifurcated caudal filaments, and a short, rounded, slightly curved pupa with squared ocular caps. These characters are partially shared with the genera *Nhambikuara*, *Pareuptychia* Forster, 1964,

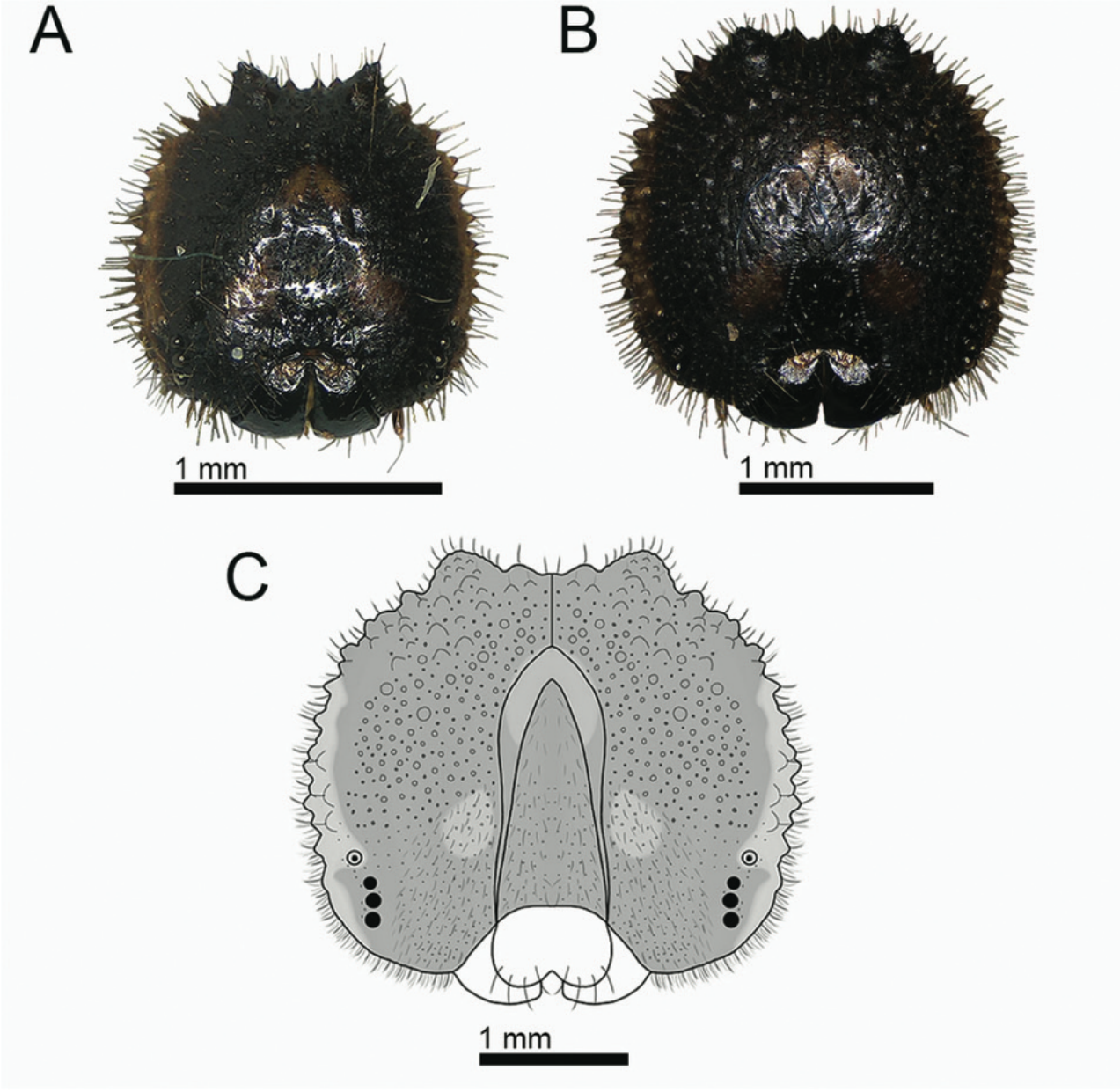

Figure 13. *Pierella hyalinus* larval head capsules collected and photographed after molting (all in frontal view): (A) antepenultimate instar; (B) penultimate instar; (C) ultimate instar (all photos are of 2025-FLP-IMM-0004).

C. chlorimene, *Godartiana muscosa* (Butler, 1870), *Taydebis melobosis*, and *Satyrotaygetis* Forster, 1964; however, notable differences are present in larval body coloration in the final instar and in head capsule morphology across all instars. The characters described above differ from those reported for *M. antonoe*, the sister species of *E. antonina* (Espeland et al. 2023), which presents yellow, unbranched caudal filaments, rounded, unbranched scoli, and a whitish body (Janzen and Hallwachs 2018).

The immature stages of *E. antonina* exhibit several characters that are unique within the Euptychiina. These include a first-instar head capsule with a corrugated, non-glossy surface; dark green bands on the posterior portion of the head capsule and beneath the scoli in lateral view from the fourth instar onward; long scoli distally bifurcated and slightly asymmetrical, with the outer branch more robust, from the third instar onward; a broad, bright yellow longitudinal subdorsal band in the final instar; turquoise-colored caudal filaments laterally in the final instar; a pupa bearing a brown, hourglass-shaped dorsal mark on the thorax; and brown margins on the ocular caps.

Several morphological traits of *M. myncea* are partially shared with other euptychiine species. For example, larvae of *Paryphthimoides brixius* (Godart, [1824]),

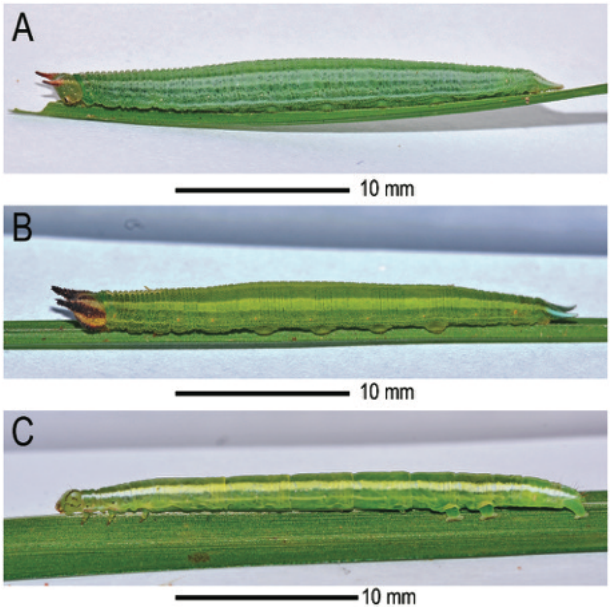

Figure 14. Morphological similarities between sedge-feeding larvae; (A) ultimate instar of *Chloreuptychia chlorimene*; (B) ultimate instar of *Erichthodes antonina*; (C) ultimate instar of an unidentified Pyralidae species.

P. poltys (Prittwitz, 1865), *P. terrestris* (Butler, 1867), and *D. ocypete* (Fabricius, 1776) exhibit divergent, unbranched horn-like scoli, head capsules lacking pronounced chalazae and with a relatively smooth surface, and robust bodies with a zigzag subdorsal band (Murray 2001; Zacca et al. 2020; Corahua-Espinoza et al. 2022a, 2022b). The short pupa with conical abdominal protuberances is similar to that reported for *M. libye* (Kaminsky and Freitas 2008) and for species of *Paryphthimoides* Forster, 1964 and *Cissia* Doubleday, 1848. Likewise, the change in body coloration in the final instar is shared with multiple species across different clades (Freitas et al. 2018; Tejeira et al. 2021; Corahua-Espinoza et al. 2022a, 2022b); however, we emphasize that the coloration in *M. myncea* is markedly darker compared with that of the other species.

The larvae of *M. myncea* follow the general pattern observed in other known species of the genus, but they also exhibit characters that may be more informative for interspecific discrimination. The egg is slightly flattened; first-instar scoli are somewhat more robust and elongated than in other Euptychiina species, with the exception of *D. ocypete*; from the second instar onward, the scoli are broad at the base, pointed at the apex, uncurved, and divergent; and the chalazae are reduced and weakly developed, dark brown body with a line of minute white dots in the subdorsal and supraspiracular regions.

Janzen and Hallwachs (2018) documented the larvae of *Pierella luna* (Fabricius, 1793) and *P. helvina incanescens* in Costa Rica, noting that in both species the larvae have a spherical head capsule with faint reddish spots in dorsal view, a pair of very short triangular scoli, a mottled brown body, very short caudal filaments, and a rounded brown pupa. Our observations show that the larvae of *P. hyalinus* exhibit a high degree of similarity to the morphology of the other two species of the genus for which life-cycle information is available. Likewise, within Haeterini, there is similarity in both head capsule shape and body coloration with *Dulcedo polita* (Janzen and Hallwachs 2018); however, marked differences are observed when compared with the larvae of *Haetera* and *Cithaerias*, which display white spots on the head capsule in the later larval instars and well-developed scoli throughout the entire life cycle (Constantino 1993; Murillo-Hiller 2009).

Possible phylogenetic implications

The phylogenetic position of *Chloreuptychia* Forster, 1964 remains somewhat unclear, with the genus appearing either as the sister group to the '*Pareuptychia* clade,' as the sister group to '*Archeuptychia* clade,' or as the sister lineage to the clade formed by the '*Taygetis* clade' + '*Splendeuptychia* clade' + '*Archeuptychia* clade' (Espeland et al. 2023). The larval traits documented in this study may help clarify these questions. For example, the immature stages of *C. chlorimene* appear to share more morphological traits with species belonging to the '*Archeuptychia* clade' and '*Pareuptychia* clade.' These similarities are present in both clades and include the unbranched scoli from the second instar, a green body in the final instar, a fully black head capsule in the second instar, an elongated body shape, and short caudal filaments (Freitas 2003; Freitas et al. 2016; Willmott et al. 2019; Corahua-Espinoza et al. 2022b), clearly contrasting with the characteristics of the '*Taygetis* clade' or '*Splendeuptychia* clade,' where the scoli, the chalazae, the shape of the head capsule, and pupal characteristics show notable differences (e.g. Murray 2001, Freitas 2017).

The complexity increases when attempting to infer the most likely affinity of *C. chlorimene* between clades '*Archeuptychia* clade' and '*Pareuptychia* clade.' On the one hand, the larvae of *C. chlorimene* show great similarity to those of *Pseudeuptychia marica* (Tejeira et al. 2021) and *P. herseis* (pers. obs.), but differ in the shape and ornamentation of the pupa. On the other hand, the pupa of *C. chlorimene* resembles that of some genera within the '*Pareuptychia*' clade, whereas the larvae,

especially in the final instar, show marked differences. It is important to note that the adults of *C. chlorimene* exhibit an iridescent blue dorsal wing coloration similar to *Pseudeuptychia*, previously considered species of *Chloreuptychia*, which, together with the morphological similarities among the larvae, suggests that it may possibly be more closely related to the '*Archeuptychia*' clade than to the '*Pareuptychia*' clade. This is consistent with one of the alternative hypotheses proposed by Espeland et al. (2023) using a dataset with four molecular markers (4GENES dataset), in which *Chloreuptychia* is recovered as the sister group to the '*Archeuptychia*' clade. Although more data on the immature stages of taxa in these clades are required for a more comprehensive analysis (e.g. a cladistic approach), the larval characteristics documented in this study, therefore, provide insights into clarifying its phylogenetic placement and improving our understanding of the evolutionary history of Euptychiina.

Currently, the genus *Erichthodes* comprises four species, but recent evidence suggests that the genus is paraphyletic due to placement of three species (*eremita*, *jovita*, and *julia*) that likely require a new genus (Espeland et al. 2023). Phylogenetic analyses place *Erichthodes* within the '*Pareuptychia* clade' as the sister lineage to the *Megeuptychia* Forster, 1964 (Espeland et al. 2023). The larvae of *E. antonina* exhibit unique traits within the '*Pareuptychia* clade' that are different from those reported for *M. antonoe* (Cramer, 1775) (DeVries 1987; Janzen and Hallwachs 2018; Araya 2025). Morphologically, *E. antonina* shows similarities in the head capsule from the second instar with *Nhambikuara furina* and *N. mima*; and the pupa exhibits characteristics similar to those of *Satyrotaygetis iris* (Corahua-Espinoza et al. 2022b). These similarities are congruent with its position within the '*Pareuptychia*' clade, although it is noteworthy that the sister lineage, *Megeuptychia*, does not share any notable morphological traits with *E. antonina*, as reported in this study (DeVries 1987; Janzen and Hallwachs 2018; Araya 2025) and the larvae exhibit a gregarious behavior that is uncommon within Euptychiina.

The first mention, to our knowledge, of the immature stages of *M. myncea* (as '*Cissia myncea*') was made by Singer et al. (1983). In that study, some characters of the immature stages were used to classify subgenera within the genus *Cissia* as then conceived. However, the similarities identified by Singer et al. (1983) are currently shared by species of *Cissia*, *Paryphthimoides*, and *Modica* (Singer et al. 1983; Murray 2001; Zacca et al. 2018, 2020; Corahua-Espinoza et al. 2022a, 2022b). Our results on the life history of *M. myncea* agree with those of Singer et al. (1983) and Murray (2001) but reveal slight differences at generic-level. We consider that characters associated with the scoli (length, shape, and ornamentation), as well as the subdorsal bands, dark brown coloration, white body spots in the last instar larva, and the pupa with rows of conical abdominal protuberances, may be used to diagnose genera. Nevertheless, we emphasize that these characters alone should not be used to delimit species, and we note that the images of the larvae provided in both Singer et al. (1983) and Murray (2001) do not allow for an exhaustive comparison, and that Murray (2001) does not clearly specify which species is referred to as *Cissia myncea*, a name that might even refer to species now placed in separate genera.

Notably, *Pierella* Westwood, 1851 lacks species with transparent wings, a character consistent with its separation from the remaining genera in the tribe Haeterini. Likewise, the immature stages of *Pierella* differ markedly from those reported for *Haetera* Fabricius, 1807 and *Cithaerias* Hübner, [1819] (Janzen and Hallwachs 2018), which may indicate the acquisition of novel morphological characters in the latter two genera, considering the high morphological similarity between *Pierella* larvae and those of *Dulcedo polita* (Hewitson, 1869) and the position as a sister group of *Pierella* relative to the other genera (Peña et al. 2006; Matos-Maraví et al. 2019). Finally, we did not find morphological characters in the larvae or pupae of *P. hyalinus* that allow interspecific discrimination within *Pierella*; however, we present the first documented record with photographs of this species under natural conditions.

Host-plant use of Cyperaceae

The immature stages of *E. antonina* have not been previously documented to our knowledge. However, larvae have been reported as accepting an epiphytic sedge climbing from trees under captive conditions (Singer and Ehrlich 1991, as '*E. erichto*'), with this being the only host plant reported for that species in that study. Our observations are in accordance with this, as all larvae and eggs found in natural conditions were recorded on *Scleria secans*, a plant that matches the habit reported by Singer and Ehrlich (1991), and at FLP is found only near 'aguajales.' In general, species within the *Pareuptychia* clade have been recorded using bamboos or grasses as host plants (e.g. Freitas et al. 2016; Willmott et al. 2019, Corahua-Espinoza et al. 2022a; Espeland et al. 2023), with at least one report available for more than 60% of the genera within the clade. The potential host-plant specialization of *E. antonina* is particularly notable considering that the

sister species, *M. antonoe*, feeds on Marantaceae (Janzen and Hallwachs 2018), and that within the *Pareuptychia* clade only two other species (*Neonympha mitchelii* French, 1889 and *Pareuptychia ocirrhoe* (Fabricius, 1776)) are known to feed on Cyperaceae (Hamm et al. 2013; Janzen and Hallwachs 2018).

Likewise, it is noteworthy that both *E. antonina* and *C. chlorimene* appears to feed exclusively on sedges representing a possible case of oligophagy, given that they have not been found feeding on any Poaceae despite years of intensive searches for immatures at FLP focusing in this family of plants. This leads to two possible evolutionary scenarios: (1) feeding on Cyperaceae may represent an adaptive novelty that allowed certain lineages within *Pareuptychia* clade to exploit new adaptive zones, or (2) if *Chloreuptychia* is considered the sister group of *Pareuptychia* clade, and since it also feeds on Cyperaceae, host-use on Cyperaceae may instead represent an ancestral state retained in certain lineages. In both scenarios, *M. antonoe* represents an unusual adaptive novelty within Euptychiina. Further research on immature stages within this group will be required to evaluate which hypothesis is more plausible.

Modica myncea has been reported to feed on *Panicum pilosum*, and *Paspalum* sp. (both grasses in Poaceae) in nature (Singer et al. 1983). Additionally, under captive conditions it has accepted eleven more species within Poaceae and two species of the family Cyperaceae (Singer and Ehrlich 1991). Our findings show that *M. myncea* can feed on *Scleria* sp. in nature, not just under captivity. It is therefore plausible to consider that *M. myncea* is a generalist species capable of feeding across different habitat types on both grasses and sedges, although it is also possible that at least some of these host plant associations represent unrecognized cryptic species.

Host plants associated with *Pierella* are usually families within the order Zingiberales, with some sporadic records on grasses and palms (Beccaloni et al. 2008; Janzen and Hallwachs 2018). The first record on Cyperaceae, an unidentified species, was reported for *P. nereis* (Brown 1992). Subsequently, *P. helvina incanescens* was documented in Costa Rica feeding on *Scleria melaleuca* Rchb. ex Schltdl. and Cham. and *S. secans* as host plants (Janzen and Hallwachs 2018). Our record on *Scleria* sp. represents the first confirmed record of a Cyperaceae as a host plant for *P. hyalinus*. We do not rule out the possibility that, in the work of Urich and Emmel (1990), the unidentified grass species on which oviposition was observed and the life cycle was recorded may in fact correspond to a species of *Scleria*, given the similarity in both habit and general morphology to some Poaceae. We consider that *P. hyalinus* occasionally use sedges as host plants, although they may not constitute their primary hosts, given that reports for *Pierella* are more frequent for Marantaceae and Heliconiaceae (DeVries 1987; Beccaloni et al. 2008; Janzen and Hallwachs 2018).

Several sedge species associated with *M. libye* have been recorded under captive conditions (Singer and Ehrlich 1991). Our record confirms that under natural conditions the species can feed on *Scleria* sp. Our observations reinforce what was reported by DeVries (1987) and Singer and Ehrlich (1991), who noted that *M. libye* has generalist habits and can use host plants from both Poaceae and Cyperaceae.

Cyperaceae are not common host plants for Satyrinae compared to Poaceae; however, they may represent a specific association with certain taxa or serve as an alternative food source for more generalist species (Singer and Ehrlich 1991; Beccaloni et al. 2008). A similar pattern has been documented in some Hesperiidae taxa, in which primarily Poaceae-feeding species occasionally use Cyperaceae as alternative host plants (Clarke 2024). The low proportion of species feeding on Cyperaceae may be related to a reduced efficiency in converting ingested food into body tissue by the larvae or due to the low energetic yield provided by the host plants, potentially leading to longer developmental cycles, and increasing the likelihood of parasitism or predation (Gomi et al. 2005; Barraclough et al. 2014; Holmes et al. 2020). In this study, we report two Euptychiina species with unusually long life cycles feeding on *S. secans*, *C. chlorimene*, and *E. antonina*. While the typical duration of life cycle among different individuals of *C. chlorimene* and other species in the study site is approximately 40 days, both *C. chlorimene* and *E. antonina* also exhibited life cycles of up to 92 and 100 days (from egg to adult), respectively, more than twice that of other Euptychiina with known immatures.

Additionally, we report a variation in the number of instars in *C. chlorimene*, presenting five larval instars when feeding on *Scleria* sp. and at least one individual went through eight larval instars when feeding on *S. secans*. It is possible that *S. secans* has low nutritional value or contains a secondary metabolite that causes larvae to undergo a greater number of instars, consequently lengthening their life cycle (Murray 2001; Mo et al. 2013; Aslan et al. 2025). Given that immatures of *C. chlorimene* are more commonly found on *Scleria* sp. than *S. secans*, it is possible that the latter sedge species is not their preferred host plant at the study site. It is likely that the association of Satyrinae with their host plants is much more complex than currently appreciated and that some groups may show high specificity in host selection.

We still do not know which factors may explain this observed specialization in some species, but it could reflect a case of adaptive speciation within the group in response to selection pressure on the use of Poaceae as host plants (Janz et al. 2006; Peña and Wahlberg 2008).

In conclusion, sedge feeding is not common within Satyrinae, and within the Euptychiina it is so far only known from small clades such as *Chloreuptychia*, *Erichthodes*, and some members of the '*Splendeuptychia* clade.' We highlight the value and the level of detail provided in our descriptions and reinforce the importance of including larval and pupal characters to understand the interactions between butterflies and their host plants. Immature stages information can also impact phylogenetic studies in lineages with unstable generic boundaries. We emphasize the substantial gaps that still exist in our understanding of the immature life histories of Satyrinae, where knowledge of immature stages continues to be poorly represented in comparative studies.

Many previous studies provide detailed descriptions of the chaetotaxy of the head capsule and body in the first instar (e.g. Freitas et al. 2018; Aguiar et al. 2025); however, many offer only limited details for later instars, which we believe may provide valuable information for delimiting groups or supporting phylogenetic relationships (see the discussion on semaphoronts in Faria et al. 2020). In addition to the apparent specialization and crypsis strategies reported herein, the repetitive and separate evolution of Cyperaceae-feeding in Euptychiina implies that sedges are ecologically significant host plants rather than incidental resources. When combined, these results highlight the ecological complexity of Satyrinae, which has previously been underestimated. We also highlight the importance of combining the morphology of immature stages with host plant associations in order to gain a thorough understanding of the dynamics of diversification and adaptive evolution in Neotropical butterflies.

Acknowledgments

We thank José Cueva, Miranda Barron, Abbye Wilkins, and Johana Reyes for their logistical support and field assistance during this research. We are also grateful to Isabel Larridon, Kenneth Bauters, and Gordon C. Tucker for their valuable help in identifying Cyperaceae species.

Author contributions

CRediT: **Yeison Vega:** Conceptualization, Data curation, Formal analysis, Investigation, Methodology, Validation, Visualization, Writing – original draft, Writing – review & editing; **Zunilda Escalante-Arteaga:** Conceptualization, Data curation, Formal analysis, Investigation, Methodology, Writing – original draft; **Karla Fiallos-Yanez:** Conceptualization, Data curation, Investigation, Validation, Writing – review & editing; **Katherine García-Luquillas:** Investigation, Methodology, Writing – review & editing; **Keith Willmott:** Supervision, Validation, Writing – review & editing; **Geoffrey Gallice:** Funding acquisition, Project administration, Resources, Supervision, Writing – review & editing; **Shinichi Nakahara:** Conceptualization, Data curation, Formal analysis, Investigation, Methodology, Supervision, Validation, Visualization, Writing – original draft, Writing – review & editing.

Disclosure statement

No potential conflict of interest was reported by the author(s)

Funding

Molecular work was funded by CONCYTEC (Peru) through the PROCIENCIA Program under the call 'Proyectos de Investigación Básica 2023-1' contract no. PE501082173-2023.

ORCID

Yeison Vega http://orcid.org/0000-0002-2492-6866
Zunilda Escalante-Arteaga http://orcid.org/0000-0002-4266-9592
Karla Fiallos-Yanez http://orcid.org/0009-0007-8940-9919
Katherine García-Luquillas http://orcid.org/0000-0003-1025-6790
Keith Willmott http://orcid.org/0000-0002-9228-0219
Geoffrey Gallice http://orcid.org/0000-0003-4381-4437
Shinichi Nakahara http://orcid.org/0000-0002-2912-343X

References

Ackery PR. 1988. Hostplants and classification: a review of nymphalid butterflies. Biol J Linn Soc. 33(2):95–203. https://doi.org/10.1111/j.1095-8312.1988.tb00446.x

Ackery PR, de Jong R, Vane-Wright RI. 1999. The butterflies: Hedyloidea, Hesperoidea and Papilionoidea. In: Kristensen NP, editor. Lepidoptera: moths and butterflies. 1. Evolution, systematics and biogeography. Handbook of zoology. Vol IV. Walter de Gruyter. p 355–401.

Aguiar TMC et al. 2025. Immature stages, population ecology and natural history of the genus Carminda Ebert & Dias (Lepidoptera: Nymphalidae: Satyrinae). Rev Bras Entomol. 69(3):e20250024.

Araya E. 2025 Nov 11. *Megeuptychia antonoe* (Nymphalidae). Área de Conservación Guanacaste. https://www.acguanacaste.ac.cr

Aslan B, Birgücü AK, Aslan EG. 2025. Impact of host switching at different larval instars on the performance of the polyphagous pest *Tuta absoluta* (Meyrick) (Lepidoptera: Gelechiidae). Sci Rep. 15(1):10803. https://doi.org/10.1038/s41598-025-94271-z

Barraclough EI, Burgess EPJ, Kean AM, Malone LA. 2014. Growth and development in a lepidopteran with variable instar number, *Pseudocoremia suavis* (Geometridae), under standard rearing conditions and when parasitised by *Meteorus pulchricornis* (Hymenoptera: Braconidae). Eur J Entomol. 111 (4):501–511. https://doi.org/10.14411/eje.2014.062

Beccaloni GW, Viloria AL, Hall SK, Robinson GS. 2008. Catalogue of the hostplants of the Neotropical butterflies. m3m-Monografias Tercer Milenio, Sociedad Entomológica Aragonesa (SEA), Red Iberoamericana de Biogeografía y Entomología Sistemática (RIBES), Ciencia y Tecnología para el Desarrollo (CYTED), Natural History Museum (NHM), Instituto Venezolano de Investigaciones Científicas.

Brown JH, Lomolino MV. 1998. Biogeography. 2nd ed. Sinauer Associates Inc. Publishers.

Brown K. 1992. Borboletas da Serra do Japi: diversidade, habitats, recursos alimentares e variação temporal. In: Morellato LPC, editor. História Natural da Serra do Japi: ecologia e preservação de uma área florestal no Sudeste do Brasil. Editora Unicamp. p 14–186.

Cardoso P, Erwin TL, Borges PAV, New TR. 2011. The seven impediments in invertebrate conservation and how to overcome them. Biol Conserv. 144(11):2647–2655. https://doi.org/10.1016/j.biocon.2011.07.024

Clarke HE. 2024. A checklist of European butterfly larval foodplants. Ecol Evol. 14(1):e10834. https://doi.org/10.1002/ece3.10834

Constantino LM. 1993. Notes on Haetera from Colombia, with description of the immature stages of Haetera piera (Lepidoptera: Nymphalidae: Satyrinae). Trop Lepid Res. 4 (1):13–14.

Corahua-Espinoza T et al. 2022a. Immature stages and new host plant records for four satyrine species feeding on herbaceous bamboos in southeastern Peru (Lepidoptera: Nymphalidae: Satyrinae: Satyrini). Zootaxa. 5125 (1):37–62. https://doi.org/10.11646/zootaxa.5125.1.3

Corahua-Espinoza T et al. 2022b. Early stage biology of two euptychiine butterfly species in the Peruvian Amazon (Lepidoptera: Nymphalidae: Satyrinae: Satyrini). Trop Lepid Res. 32(1):38–46.

DeVries PJ. 1986. Hostplant records and natural history notes on Costa Rican butterflies (Papilionidae, Pieridae and Nymphalidae). J Res Lepid. 24(4):290–333. https://doi.org/10.5962/p.266791

DeVries PJ. 1987. The butterflies of Costa Rica and their natural history. Princeton University Press.

Diniz-Filho JAF, Loyola RD, Raia P, Mooers AO, Bini LM. 2013. Darwinian shortfalls in biodiversity conservation. Trends Ecol Evol. 28(12):689–695. https://doi.org/10.1016/j.tree.2013.09.003

Espeland M et al. 2019. Four hundred shades of brown: higher level phylogeny of the problematic Euptychiina (Lepidoptera, Nymphalidae, Satyrinae) based on hybrid enrichment data. Mol Phylogenet Evol. 131:116–124. https://doi.org/10.1016/j.ympev.2018.10.039

Espeland M et al. 2023. Combining target enrichment and Sanger sequencing data to clarify the systematics of the diverse Neotropical butterfly subtribe Euptychiina (Nymphalidae, Satyrinae). Syst Entomol. 48(4):498–570. https://doi.org/10.1111/syen.12590

Faria LRR, Pie MR, Salles FF, Soares EDG. 2020. The Haeckelian shortfall or the tale of the missing semaphoronts. J Zool Syst Evol Res. 59(2):359–369. https://doi.org/10.1111/jzs.12435

Folmer O, Black M, Hoeh W, Lutz R, Vrijenhoek R. 1994. DNA primers for amplification of mitochondrial cytochrome c oxidase subunit I from diverse metazoan invertebrates. Mol Mar Biol Biotechnol. 3(5):194–299.

Fortier RP, Corahua-Espinoza T, Swamy V, Feeley KJ, Gallice GR. 2025. Insights from a New 1-ha permanent forest plot reveal differences between habitat type and similarities between forest type in the southwestern Amazon. Ecol Evol. 15(5):e71476. https://doi.org/10.1002/ece3.71476

Freitas AVL. 2003. Description of a new genus for "*Euptychia*" *peculiaris* (Nymphalidae: Satyrinae): immature stages and systematic position. J Lepid Soc. 57 (2):100–106.

Freitas AVL 2017. Immature stages of Neotropical satyrine butterfly *Taygetis acuta* (Nymphalidae: euptychiina). Trop Lepid Res. 27(1):1–5.

Freitas AVL. 2022. Immature stages of *Splendeuptychia ambra* (Nymphalidae: Euptychiina) and the diversity of immature morphology within *Splendeuptychia*. Trop Lepid Res. 32(1):52–58.

Freitas AVL et al. 2018. Immature stages of two *Moneuptychia* from southeastern Brazil (Nymphalidae: Euptychiina). Trop Lepid Res. 28(2):100–105.

Freitas AVL, Brown KS. 2004. Phylogeny of the Nymphalidae (Lepidoptera). Syst Biol. 53(3):363–383. https://doi.org/10.1080/10635150490445670

Freitas AVL, Carreira JYO, Santos JP, Barbosa EP. 2016. Immature stages and natural history of two species of *Forsterinaria* from southeastern Brazil (Lepidoptera: Nymphalidae). Trop Lepid Res. 26(1):13–18.

García-Barros E, Martín J. 1995. The eggs of European satyrine butterflies (Nymphalidae): external morphology and its use in systematics. Zool J Linn Soc. 115(1):73–115. https://doi.org/10.1006/zjls.1995.0034

Gomi T, Hirochika M, Nagasaka M, Hagihara H, Fukuda T. 2005. Effects of diet on life-history traits in a trivoltine Kobe population of *Hyphantria cunea* (Drury) (Lepidoptera: Arctiidae). Appl Entomol Zool. 40 (3):475–482. https://doi.org/10.1303/aez.2005.475

Greeney HF, Pyrcz TW, Dyer LA, Sánchez ZM, Walla TR. 2010. The early stages and natural history of *Corades medeba* Hewitson, 1850 in eastern Ecuador (Lepidoptera: Nymphalidae: Satyrinae: Pronophilina). Trop Lepid Res. 20(1):8–13.

Hamm CA, Williams BL, Landis DA. 2013. Natural history and conservation status of the endangered Mitchell's satyr butterfly: synthesis and expansion of our knowledge regarding *Neonympha mitchellii mitchellii* French 1889. J Lepid Soc. 67 (1):15–28. https://doi.org/10.18473/lepi.v67i1.a2

Hebert PDN, Penton EH, Burns JM, Janzen DH, Hallwachs W. 2004. Ten Species in one: DNA barcoding reveals cryptic species in the neotropical skipper butterfly *Astraptes fulgerator*. Proc Natl Acad Sci USA. 101(41):14812–14817. https://doi.org/10.1073/pnas.0406166101

Holmes LA, Nelson WA, Lougheed SC. 2020. Food quality effects on instar-specific life histories of a holometabolous insect. Ecol Evol. 10(2):626–637. https://doi.org/10.1002/ece3.5790

Hurtado T et al. 2021. Complete immature stages of the euptychiine butterfly *Taygetis cleopatra* (C. Felder and R. Felder, 1862) (Lepidoptera: Nymphalidae: Satyrinae) in southeastern Peru. Trop Lepid Res. 31(3):179–185.

Janz N, Nylin S, Wahlberg N. 2006. Diversity begets diversity: host expansions and the diversification of plant-feeding insects. BMC Evol Biol. 6(4). https://doi.org/10.1186/1471-2148-6-4

Janzen DH, Hallwachs W. 2018. Dynamic database for an inventory of the Macrocaterpillar Fauna, and its food plants and parasitoids, of the area de Conservacion Guanacaste (ACG). Northwestern Costa Rica. University of Pennsylvania; [accessed 2021 Oct 18]. http://janzen.sas.upenn.edu

Kaminski LA, Freitas AVL. 2008. Immature stages of the butterfly *Magneuptychia libye* (L.) (Lepidoptera: Nymphalidae, Satyrinae). Neotrop Entomol. 37(2):169–172. https://doi.org/10.1590/S1519-566X2008000200010

Katoh K, Rozewicki J, Yamada KD 2019. MAFFT online service: multiple sequence alignment, interactive sequence choice and visualization. Brief Bioinform. 20(4):1160–1166. https://doi.org/10.1093/bib/bbx108

Kitching IJ. 1984. The use of larval chaetotaxy in butterfly systematics, with special reference to the Danaini (Lepidoptera: Nymphalidae). Syst Entomol. 9:49–61. https://doi.org/10.1111/j.1365-3113.1984.tb00500.x

Kumar S, Stecher G, Tamura K 2016. MEGA7: molecular evolutionary genetics analysis version 7.0 for bigger datasets. Mol Biol Evol. 33(7):1870–1874. https://doi.org/10.1093/molbev/msw054

Larsson A 2014. AliView: a fast and lightweight alignment viewer and editor for large datasets. Bioinformatics. 30(22):3276–3278. https://doi.org/10.1093/bioinformatics/btu531

Lin RJ, Braby MF, Hsu YF. 2019. The immature stages, biology, and phylogenetic relationships of *Rotunda rotundapex* (Lepidoptera: Bombycidae). J Insect Sci. 19(2):1–11. https://doi.org/10.1093/jisesa/iez025

Lomolino MV. 2004. Conservation biogeography. In: Lomolino M, Heaney L, editors. Frontiers of biogeography: new directions in the geography of nature. Sinauer Associates. p 293–296.

Matos-Maraví P, Wahlberg N, Antonelli A, Penz CM. 2019. Species limits in butterflies (Lepidoptera: Nymphalidae): reconciling classical taxonomy with the multispecies coalescent. Syst Entomol. 44(4):745–756. https://doi.org/10.1111/syen.12352

Mo HH et al. 2013. Interactive effect of diet and temperature on instar numbers in *Spodoptera litura*, with reference to head capsule width and weight. J Asia-Pac Entomol. 16(3):377–383. https://doi.org/10.1016/j.aspen.2013.08.007

Montero F, Ortiz M. 2012. Estados inmaduros e historia natural de algunas especies de la subtribu Pronophilina (Nymphalidae: Satyrinae) presentes en el páramo del Tablazo — Colombia. II. *Lymanopoda schmidti* Adams, 1986. Trop Lepid Res. 22(2):100–109.

Montero F, Ortiz M. 2014. Ciclo de vida de *Corades chelonis* Hewitson y *Corades dymantis* Thieme (Lepidoptera: Nymphalidae: Satyrinae: Pronophilina) y aspectos de su biología. Insecta Mundi. 345:1–29.

Murillo-Hiller LR. 2009. Early stages and natural history of *Cithaerias p. pireta* (Satyrinae) from Costa Rica. J Lepid Soc. 63(3):169–172.

Murray DL. 2001. Systematics of euptychiine butterflies (Nymphalidae: Satyrinae: Euptychiina) based on larval morphology and DNA sequence data and the evolution of life history traits. Louisiana State University.

Otero LS, Casagrande MM. 1992. Hibridismo em Brassolinae (Lepidoptera, Nymphalidae). Rev Bras Entomol. 36(4):723–728.

Otero LS, Marigo LC. 1990. Butterflies. Beauty and behavior of Brazilian species. Marigo Comunicação Visual.

Padrón P, Boyer P, Vélez A, Pyrcz T. 2019. Description of the immature stages of a rare Andean paramo butterfly *Lymanopoda caracara* Pyrcz, Willmott and J. Hall, 1999 (Lepidoptera: Nymphalidae). Zool Syst. 44(4):316–324. https://doi.org/10.11865/zs.201930

Peña C et al. 2006. Higher level phylogeny of Satyrinae butterflies (Lepidoptera: Nymphalidae) based on DNA sequence data. Mol Phylogenet Evol. 40(1):29–49.

Peña C, Wahlberg N. 2008. Prehistorical climate change increased diversification of a group of butterflies. Biol Lett. 4(3):274–278. https://doi.org/10.1098/rsbl.2008.0062

Penz CM, Peggie D. 2003. Phylogenetic relationships among heliconiinae genera based on morphology (Lepidoptera: Nymphalidae). Syst Entomol. 28(4):451–479. https://doi.org/10.1046/j.1365-3113.2003.00221.x

Pyrcz TW, Wojtusiak J. 2002. The vertical distribution of pronophiline butterflies (Nymphalidae, Satyrinae) along an elevational transect in Monte Zerpa (Cordillera de Mérida, Venezuela) with remarks on their diversity and parapatric distribution. Glob Ecol Biogeogr. 11(3):211–221. https://doi.org/10.1046/j.1466-822X.2002.00285.x

Schneider CA, Rasband WS, Eliceiri KW. 2012. NIH image to ImageJ: 25 years of image analysis. Nat Methods. 9(7):671–675. https://doi.org/10.1038/nmeth.2089

Shin SK, Lee Y, Kwon H, Rhee JS, Kim JK. 2021. Validation of direct boiling method for simple and efficient genomic DNA extraction and PCR-based macroalgal species determination. J Phycol. 57(4):1368–1372. https://doi.org/10.1111/jpy.13175

Singer MC, DeVries PJ, Ehrlich PR. 1983. The *Cissia confusa* species-group in Costa Rica and Trinidad (Lepidoptera: Satyrinae). Zool J Linn Soc. 79(2):101–119. https://doi.org/10.1111/j.1096-3642.1983.tb01162.x

Singer MC, Ehrlich PR. 1991. Host specialization of satyrine butterflies, and their responses to habitat fragmentation in Trinidad. J Res Lepid. 30(3–4):248–256. https://doi.org/10.5962/p.266650

Srivathsan A, Feng V, Suárez D, Emerson B, Meier R. 2023. Ontbarcoder 2.0: rapid species discovery and identification with real-time barcoding facilitated by Oxford Nanopore R10.4. Cladistics. 40(2):192–203. https://doi.org/10.1111/cla.12566

Srivathsan A, Meier R. 2024. Scalable, cost-effective, and decentralized DNA barcoding with Oxford Nanopore sequencing. Methods Mol Biol. 2744:223–238. https://doi.org/10.1007/978-1-0716-3581-0_14

Stehr FW. 1987. Order Lepidoptera. In: Stehr FW, editor. Immature insects. Vol I. Kendall/Hunt Publishing. p 293–294.

Tejeira R et al. 2021. Immature stages of *Chloreuptychia marica* (Weymer, 1911) (Lepidoptera: Nymphalidae: Satyrinae: Satyrini). Trop Lepid Res. 31(2):96–100.

Urich FC, Emmel TC. 1990. Life histories of neotropical butterflies from Trinidad 2. *Antirrhaea philoctetes* (Lepidoptera: Nymphalidae: Morphinae). Trop Lepid Res. 1(1):27–32.

Willmott KR et al. 2019. A revision of the new Andean butterfly genus *Optimandes* Marín, Nakahara and Willmott, n. gen. with the description of a new species (Nymphalidae: Satyrinae: Euptychiina). Trop Lepid Res. 29(1):29–44.

Young AM. 1984. Natural history notes for *Taygetis andromeda* (Cramer) (Satyrinae) in Eastern Costa Rica. J Lepid Soc. 38:102–113.

Zacca T et al. 2018. Systematics of the butterfly genus *Cissia* Doubleday, 1848 (Lepidoptera: Nymphalidae: Satyrinae) using an integrative approach. Arthropod Syst Phylog. 76(2):349–376. https://doi.org/10.3897/asp.76.e31933

Zacca T et al. 2020. Systematics of the Neotropical butterfly genus *Paryphthimoides* Forster, 1964 (Lepidoptera: Nymphalidae: Satyrinae), with descriptions of seven new taxa. Insect Syst Evol. 52(1):42–96. https://doi.org/10.1163/1876312X-00001027

Zacca T, Barbosa EP, Freitas AVL. 2018. Euptychiina species checklist. Universidade Estadual de Campinas. https://labbor.ib.unicamp.br/?page_id=1020